ARC Centre of Excellence in Population Ageing Research

Working Paper 2021/22

Valuation of guaranteed minimum maturity benefits under generalised regime-switching models using the Fourier Cosine method

Boda Kang, Yang Shen, Dan Zhu and Jonathan Ziveyi

Valuation of guaranteed minimum maturity benefits under generalised regime-switching models using the Fourier Cosine method

Boda Kang[*] Yang Shen[†] Dan Zhu[‡] and Jonathan Ziveyi[§]

July 15, 2021

Abstract

This paper presents a flexible valuation approach for variable annuity (VA) contracts embedded with guaranteed minimum maturity benefit (GMMB) riders written on an underlying fund that evolves according to a general regime-switching framework. Unlike the classical regime-switching models which only allow model parameters to change upon regime switches, our framework allows, more importantly, model structures to vary. With mild assumptions on the characteristic function of the log-stock price, our model settings enable the study of fundamental features of the market dynamics, such as stochastic volatility and jumps, on the underlying fund value of GMMB in a unified framework. This novel idea is illustrated by a three-regime model whose environments can be characterised by either the geometric Brownian motion process, double exponential process or the Heston (1993) stochastic volatility process. Two versions of the GMMB riders are considered; a fixed or roll-up guarantee and a ratchet geometric average guarantee. With the Fourier Cosine (COS) method which utilises characteristic functions, explicit valuation expressions for various contracts are derived, and numerical illustrations are performed to analyse the efficiency of the approach in terms of computational speed and accuracy. The paper makes a unique contribution by presenting regime-dependent bounds and an algorithm for determining the optimal grid points required for the COS method to achieve a specific level of accuracy. Numerical experiments for the valuation framework reveal that as the likelihood of regime shifts increases, the price difference of VA contracts with different initial regimes diminishes, which is consistent with financial intuition.

JEL Classification: C63, G12, G22, G23

Keywords: Variable annuity contracts; GMMB; COS method; Generalised regime-switching model; Ratchet options

[*]boda_kang@amp.com.au; AMP; 33 Alfred Street, Circular Quay, Sydney, NSW 2000, Australia.

[†]Corresponding Author: y.shen@unsw.edu.au; School of Risk and Actuarial Studies, ARC Centre of Excellence in Population Ageing Research (CEPAR), University of New South Wales, Sydney, NSW 2052, Australia. Yang acknowledges the financial support of the Australian Research Council Discovery Early Career Researcher Award DE200101266 Demystifying Puzzles in Retirement Planning.

[‡]dan.zhu@monash.edu; Department of Econometrics and Business Statistics, Monash University, Caulfield East, 3145, Australia.

[§]j.ziveyi@unsw.edu.au; School of Risk and Actuarial Studies, CEPAR, UNSW, Sydney, NSW 2052, Australia. Jonathan acknowledges the financial support of the Australian Research Council Discovery Grant Project DP170102275 Retirement Income Product Innovation.

1 Introduction

Variable annuities (VAs) have become part of retirement portfolios for many retirees. Compared with traditional fixed annuities, one distinguishing feature of variable annuities is that they are equity-linked insurance products and usually embedded with guaranteed minimum benefits (GMBs) in the event of poor market performance. The popularity of VAs among retirees is primarily due to a range of investment options and downside risk protection offered by embedded guarantees, frequently referred to as riders. These riders can be categorised into two classes namely; guaranteed minimum death benefits (GMDBs) and guaranteed minimum living benefits (GMLBs). A GMDB rider provides a guaranteed death benefit to the policyholder's beneficiary if the policyholder dies during the contract term. GMLBs encompass a wide range of riders which include guaranteed minimum maturity benefit (GMMB), guaranteed minimum income benefit (GMIB), and guaranteed minimum withdrawal benefit (GMWB). With a GMMB rider, the policyholder is promised a guaranteed amount upon maturity of the contract in the event of poor market conditions. A GMIB promises periodic payments upon annuitisation of a GMMB whilst a GMWB rider guarantees withdrawal of at least the initial investment during the tenure of the contract.

VAs are usually long-dated contracts whose maturities can extend for several decades. Though the pricing of GMBs has been extensively studied in the literature, most works assume that the underlying asset dynamics follow the geometric Brownian motion (GBM) model. This assumption significantly simplifies the valuation framework and makes it possible to obtain analytical pricing formulas (Bauer et al., 2008; Dai et al., 2008; Feng and Jing, 2017; Milevsky and Salisbury, 2006; Shen et al., 2016). Recently, there has been increasing interest in departing from the classic GBM paradigm and considering the valuation of GMBs under more realistic models. The first direction is based on diffusion-driven financial market models with Dai et al. (2015) considering the pricing of GMWBs and guaranteed lifetime withdraw benefits (GLWBs) under a framework with stochastic interest rate and stochastic mortality. Several extensions have been proposed along this direction (Deelstra and Rayée, 2013; Da Fonseca and Ziveyi, 2017; Gudkov et al., 2019; Kang and Ziveyi, 2018; Shevchenko and Luo, 2017). The second direction involves modelling underlying fund dynamics using Lévy processes. Kélani and Quittard-Pinon (2017) develop a general methodology for pricing and hedging VAs in a Lévy market from the risk management perspective. Alonso-García et al. (2018) apply the Fourier-cosine method to the pricing and hedging of GMWB riders. Ballotta et al. (2020) propose a market consistent valuation framework for VAs in a hybrid Levy model with dependent surrender risk.

While these extensions are interesting in analysing GMBs, neither diffusion-driven models nor Lévy-based models can capture the structural changes in the underlying asset price dynamics due to fluctuating macroeconomic conditions, altering the fundamentals of financial markets. Hence, the works mentioned above have ignored the long-term feature of VA contracts and may cause significant underestimation of the actual value of those optional guarantees in VAs. In an empirical study of vanilla options under regime-switching models, Shen et al. (2014) find that ignoring regime-switching risk (that is, macroeconomic risk) would result in over 6% underestimation of option prices. Indeed, regime-switching models are ideal candidates for characterising

long-dated options like VAs with guarantees.

As such, the third research direction utilises regime-switching models to capture the macroeconomic risk inherent in markets. Fan et al. (2015) consider the pricing of equity-indexed annuities and GMDBs under a double regime-switching model by using the fast Fourier transform method. Using the Fourier space time-stepping algorithm, Ignatieva et al. (2016, 2018) study the pricing and hedging of GMBs under the regime-switching and stochastic mortality models. Mamon et al. (2020) investigate the valuation of GMMBs under a hidden Markov model by employing the Fourier transform method and recursive filtering technique.

In this paper, we consider the valuation of a VA contract embedded with GMMB riders, which is the foundation for the pricing of GMIB and GMDB riders. We focus on the GMMB benefits with three payoff functions, including fixed, rolled up, and geometric average guarantees. To model the dynamics of the underlying fund, we develop a novel class of regime-switching models, namely, generalised regime-switching (GRS) models, which extend the classical regime-switching (CRS) models (Elliott et al., 2005) to a more general set-up. This extension is a stand-alone contribution to the paper. Under a CRS model, after regime shifts, only the values of model parameters will change, and the model structure remains the same. For instance, in Elliott et al. (2005), the stock price is always described by the geometric Brownian motion (GBM) model in each state with state-dependent parameters, such as risk-free interest rate, expected return, and volatility. Whereas in a GRS model, upon regime shifts, not only the values of model parameters vary, but also the model structure may as well change. For instance, in Example 2.1 of this paper, before a transition, the stock price process may evolve according to the GBM model with constant volatility; after a transition, it would turn out to be a new stock price model with stochastic volatility, such as the Heston (1993) model. Our model setting is general in the sense that we only require that the characteristic function of the log-stock price satisfies a structural assumption and do not need to specify the price dynamics from the very beginning. This allows us to incorporate a range of regime-switching models with structural changes. Indeed, besides regime-switching, our model can also capture other important features of financial markets, such as jumps, stochastic volatility, and stochastic interest rate.

Our second main contribution is to develop a Fourier Cosine (COS) algorithm to price VA contracts by utilising the corresponding characteristic function. The implementation of the COS method is non-trivial. One novelty in our algorithm is a set of ingenious regime-dependent bounds used in the approximation procedure of the COS method. To find those regime-dependent bounds, we define and derive a generalised characteristic function allowing for a Markov-modulated domain. The regime-dependent bounds distinguish our COS algorithm from the existing works, in which the bounds are constant. See, for example, Alonso-García et al. (2018), Chau et al. (2015), Fang and Oosterlee (2008), Li et al. (2021), and Tour et al. (2018). With this innovation, our COS algorithm outperforms the Monte Carlo method in terms of computation time. In the COS method, we demonstrate that the logarithm of the absolute value of error has a linear relationship with the logarithm of the grid size.

We present a thorough sensitivity analysis of the VA contract prices with respect to various model parameters under our newly introduced framework. All observed trends are consistent with financial intuition. In particular, as the likelihood of regime shifts increases, the difference of the VA contract prices with different initial regimes

will diminish. In other words, for different initial regimes, the VA contract prices will either increase or decrease as the transition intensity changes. This price sensitivity implies that the misspecification of the transition matrix may have an ambiguous impact on the VA contract prices and should be discussed with more caution, especially in a good initial regime.

The rest of the paper is structured as follows. In Section 2, we introduce the GRS models followed by two examples. Section 3 gives a brief review of the COS method. In Section 4, we apply the COS method to derive valuation expressions for GMMB benefits with fixed, rolled up, and geometric average guarantees. In Section 5, we implement several numerical examples highlighting our findings. Section 6 provides concluding remarks of the paper. A brief review of the CRS models is provided in Appendix A. All technical proofs are relegated to Appendix B.

2 Model setup: Generalised regime-switching models

In this section, we introduce a generalised regime-switching (GRS) framework. In the GRS framework, model parameters and model structures are both modulated by a Markov chain. In such a setting, the GRS framework is more general than the classical regime-switching (CRS) model, which has been predominantly considered in literature (Elliott et al., 2005; Fan et al., 2015; Mamon et al., 2020; Tour et al., 2018). We briefly review the CRS model in Appendix A for convenience.

We fix a probability space $(\Omega, \mathcal{F}, \mathbb{F}, Q)$ satisfying the usual conditions. The filtration, $\mathbb{F} := \{\mathcal{F}_t\}_{t\in[0,T]}$, is a natural filtration generated by all random objects to be considered in the paper and augmented in the usual way, and Q is a risk-neutral probability measure with the expectation operation denoted by $\mathbb{E}^Q[\cdot]$. One may also start from a real-world probability measure and choose a risk-neutral measure for pricing purpose via Esscher transform techniques (Elliott et al., 2005; Shen et al., 2014). Let $\{\alpha_t\}_{t\in[0,T]}$ be a Markov chain on $(\Omega, \mathcal{F}, \mathbb{F}, Q)$. By convention, we adopt the canonical representation of the Markov chain and assume that the chain α takes values in the set of standard unit vectors $\{e_1, e_2, \ldots, e_n\}$, where e_i is the i^{th} unit (column) vector of the space $\mathbb{R}^n$. Let $A := [a_{ij}]_{i,j=1,2,\ldots,n}$ be the transition rate matrix of the chain, where a_{ij} denotes the instantaneous transition rate of the chain α from state e_j to state e_i, satisfying $a_{ij} \geq 0$, for $i \neq j$; $a_{ii} \leq 0$, for $i = 1, 2, \ldots, n$; and $\sum_{i=1}^n a_{ij} = 0$, for $j = 1, 2, \ldots, n$. With the canonical state space representation, the Markov chain can be decomposed as follows

$$\alpha_t = \alpha_0 + \int_0^t A\alpha_s ds + m_t, \tag{2.1}$$

where $\{m_t\}_{t\in[0,T]}$ is an $\mathbb{R}^n$-valued martingale (Elliott et al., 1994). Obviously, for any $s \geq t$, we have

$$\mathbb{E}^Q[\alpha_s|\alpha_t] = \exp\{A(s-t)\}\alpha_t, \tag{2.2}$$

where $\mathbb{E}^Q[\cdot|\alpha_t]$ denotes an conditional expectation given α_t. This result will be used throughout the paper. Denote by $\mathbb{G} := \{\mathcal{G}_t\}_{t\in[0,T]}$ the natural filtration generated by all other random objects except the Markov chain α. Then, the filtration $\mathbb{F} = \{\mathcal{F}_t\}_{t\in[0,T]}$ is defined by

$$\mathcal{F}_t := \mathcal{G}_t \vee \mathcal{F}_t^{\alpha}, \tag{2.3}$$

where $\mathcal{F}_t^{\alpha}$ is the σ-field generated by the Markov chain α. Let $\{S_t\}_{t\in[0,T]}$ denote the stock price process with initial price $S_0 = s_0$, and $\{X_t\}_{t\in[0,T]}$ denote the log-stock price process:

$$X_t := \log(S_t), \tag{2.4}$$

with initial value $X_0 = x_0 = \log(S_0)$. Suppose that the risk-free interest rate is modulated by the chain as

$$r_t := r(\alpha_t) = \langle r, \alpha_t \rangle , \tag{2.5}$$

where

$$r := (r_1, r_2, \ldots, r_n)^{\top}, \tag{2.6}$$

and the risk-free interest rate r_t is equal to the j^{th} entry $r_j := r(e_j)$ if and only if the chain α_t is in the j^{th} state, that is, $\alpha_t = e_j$, for any $j = 1, 2, \ldots, n$. Here and throughout the paper, the inner product operator of two vectors a and b is computed as $\langle a, b\rangle = a^{\top}b$.

Under the GRS model, the log-stock process $\{X_t\}_{t\in[0,T]}$ follows

$$X_t = X_0 + \sum_{j=1}^{n} \int_0^t \langle \alpha_s, e_j \rangle \, dX_s^j. \tag{2.7}$$

Here, each $\{X_t^j\}_{t\in[0,T]}$ denotes one state of the log-stock price corresponding to the j^{th} state/regime of the Markov chain, for $j = 1, 2, \ldots, n$, since $dX_t = dX_t^j$ if and only if $\alpha_t = e_j$. Suppose that all the $\{X_t^j\}_{t\in[0,T]}$ are Markov processes adapted to $\mathbb{G}$, for $j = 1, 2, \ldots, n$, and they are stochastically independent of the Markov chain α.

Next, we construct a regime-switching stochastic factor

$$\zeta_t := \sum_{j=1}^{n} \langle \alpha_0, e_j \rangle \, \zeta_0^j + \sum_{j=1}^{n} \int_0^t \langle \alpha_s, e_j \rangle \, d\zeta_s^j, \tag{2.8}$$

which can be used to describe various stochastic factors in the stock price model, such as stochastic volatility, stochastic correlation, and stochastic jump intensity, among others. Note that the pairs of X_t^j and ζ_t^j, for $j = 1, 2, \ldots, n$, and that of X_t and ζ_t are allowed to be correlated in our framework. One can refer to Examples 2.1 and 2.2 for possible correlation structures.

Suppose that the characteristic function of $\{X_t^j\}_{t\in[0,T]}$ satisfies the following exponential form

$$\Phi^j(u; t, x^j, \zeta^j) = \mathbb{E}^Q\left[e^{iuX_T^j} | X_t^j = x^j, \zeta_t^j = \zeta^j\right] = \exp\left\{iux^j + g^j(u,t) + D(u,t,\zeta^j)\right\}, \tag{2.9}$$

under each regime $j = 1, 2, \ldots, n$, where $\mathbb{E}^Q\left[\, \cdot \, | X_t^j = x^j, \zeta_t^j = \zeta^j\right]$ denotes the conditional expectation given $X_t^j = x^j$ and $\zeta_t^j = \zeta^j$, and $g^j(u,t)$ and $D(u,t,\zeta^j)$ are deterministic functions satisfying:

i. $D(u, T, \zeta^j) = 0$, for any $(u, \zeta^j) \in \mathbb{R}^2$;

ii. $g^j(u, \cdot) \in \mathcal{C}^1([0,T])$ and $D(u, \cdot, \cdot) \in \mathcal{C}^{1,2}([0,T] \times \mathbb{R})$, for any $u \in \mathbb{R}$.

To apply the Fourier Cosine (COS) method which will be adopted for numerical implementations in this paper, we derive the (discounted) characteristic function of the log-stock price in the next proposition.

Proposition 2.1. *The discounted characteristic function of the log-stock price X_T can be represented as*

$$\begin{aligned}\widetilde{\Phi}_{X_T}(u;t,x,\zeta) &:= \mathbb{E}^Q\big[e^{-\int_t^T r_s ds + iuX_T}|X_t = x, \zeta_t = \zeta\big] \\ &= e^{iux+D(u,t,\zeta)}\left\langle \alpha_t, \Psi(u,t)1_n\right\rangle, \end{aligned} \tag{2.10}$$

where $\mathbb{E}^Q\big[\,\cdot\,|X_t = x, \zeta_t = \zeta\big]$ denotes the conditional expectation given $X_t = x$ and $\zeta_t = \zeta$ and $\Psi(u,t)$ is the fundamental solution of the following matrix-valued ordinary differential equation (ODE):

$$\frac{d\Psi(u,t)}{dt} = \big[-Diag(G(u,t)+r) + A\big]\Psi(u,t), \quad \Psi(u,T) = I_n, \tag{2.11}$$

with

$$G(u,t) := \big(g_t^1(u,t), g_t^2(u,t), \ldots, g_t^n(u,t)\big)^\top.$$

Here 1_n denotes an n-dimensional vector with all entries being one, I_n is an $n\times n$ identity matrix, and for any vector C the operator Diag$[C]$ returns a diagonal matrix with C on its diagonal.

If $g_t^j(u,t)$ are independent of t, for $j = 1,2,\ldots,n$, that is, $G(u,t) = G(u)$, for any $t\in[0,T]$, then the fundamental solution can be represented by a matrix exponential:

$$\Psi(u,t) = \exp\big\{\big[-Diag(G(u)+r) + A\big](T-t)\big\}, \tag{2.12}$$

and the characteristic function has the following closed-form expression:

$$\widetilde{\Phi}_{X_T}(u;t,x,\zeta) = e^{iux+D(u,t,\zeta)}\left\langle \alpha_t, \exp\big\{\big[-Diag(G(u)+r) + A\big](T-t)\big\}1_n\right\rangle. \tag{2.13}$$

Proof. Refer to Appendix B.1. □

With the COS method, an essential step is to approximate integrals over the infinite interval to those over a finite interval. Thus, one needs to choose an upper bound and a lower bound. One of the innovations of the paper is to implement regime-specific bounds. To this end, we define a generalised characteristic function with u in Equation (2.10) replaced by a regime-dependent u_T and (2.10) scaled by a regime-dependent B_T, where u_T and B_T are

$$u_T := u(\alpha_T) = \langle \mathbf{u}, \alpha_T\rangle, \quad B_T := B(\alpha_T) = \langle \mathbf{B}, \alpha_T\rangle, \tag{2.14}$$

with

$$\mathbf{u} := (u_1, u_2, \ldots, u_n)^\top, \quad \mathbf{B} := (B_1, B_2, \ldots, B_n)^\top. \tag{2.15}$$

That is,

$$\widehat{\Phi}_{X_T}(\mathbf{u},\mathbf{B};t,x,\zeta) := \mathbb{E}^Q\big[e^{-\int_t^T r_s ds + iu_T X_T}B_T|X_t = x, \zeta_t = \zeta\big]. \tag{2.16}$$

The following corollary is an immediate consequence of Proposition 2.1.

Corollary 2.1. *The generalised characteristic function can be represented as*

$$\widehat{\Phi}_{X_T}(\mathbf{u}, \mathbf{B}; t, x, \zeta) = \left\langle \exp\{A(T-t)\}\alpha_t, \widehat{\mathbf{\Psi}}(t, x, \zeta, \alpha_t) \right\rangle, \tag{2.17}$$

where

$$\widehat{\mathbf{\Psi}}(t, x, \zeta, \alpha_t) := \left(\widehat{\Psi}_1(t, x, \zeta, \alpha_t), \widehat{\Psi}_2(t, x, \zeta, \alpha_t), \ldots, \widehat{\Psi}_n(t, x, \zeta, \alpha_t)\right)^\top \tag{2.18}$$

with

$$\widehat{\Psi}_j(t, x, \zeta, \alpha_t) := e^{iu_j x + D(u_j, t, \zeta)} \langle \alpha_t, \Psi(u_j, t) 1_n \rangle B_j. \tag{2.19}$$

Proof. Refer to Appendix B.2. □

In what follows, we illustrate our idea of the GRS model with two examples. For this purpose, we formally define $\{W_t\}_{t\in[0,T]}$ and $\{\bar{W}_t\}_{t\in[0,T]}$ as two standard Brownian motions and $N(dt, dx)$ as the differential form of a random measure on $([0,T] \times \mathbb{R}_0, \mathcal{B}([0,T]) \otimes \mathcal{B}(\mathbb{R}_0))$, where $\mathbb{R}_0 := \mathbb{R} \setminus \{0\}$, and $\mathcal{B}([0,T])$ and $\mathcal{B}(\mathbb{R}_0)$ denote the Borel σ-fields generated by $[0,T]$ and $\mathbb{R}_0$, respectively. By convention, we assume that W, $\bar{W}$, N and α are stochastically independent. Moreover, we assume that the compensator of $N(dt, dy)$ is given by a Markov-modulated Lévy measure $\nu(dy, \alpha_t)$ as follows:

$$\pi(dt, dy, \alpha_t) := \nu(dy, \alpha_t)dt. \tag{2.20}$$

Thus, $\nu(dy, \alpha_t) = \nu(dy, e_j)$ if and only if the Markov chain is in the j^{th} state, that is, $\alpha_t = e_j$. This is mathematically equivalent to

$$\nu(dy, \alpha_t) = \langle \nu(dy), \alpha_t \rangle, \quad \nu(dy) := (\nu_1(dy), \nu_2(dy), \ldots, \nu_n(dy))^\top.$$

Then, the compensated random measure, denoted by $\widetilde{N}(dt, dy, \alpha_t)$, satisfies

$$\widetilde{N}(dt, dy, \alpha_t) = N(dt, dy) - \pi(dt, dy, \alpha_t) = N(dt, dy) - \nu(dy, \alpha_t)dt. \tag{2.21}$$

Whenever there is no risk of confusion, we simply write $\widetilde{N}_j(dt, dy) := \widetilde{N}(dt, dy, e_j)$ and $\nu_j(dy) := \nu(dy, e_j)$, for $j = 1, 2, \ldots, n$.

In the first example, the stock price follows a 3-state regime-switching model.

Example 2.1. *The log-stock price process satisfies*

$$X_t = X_0 + \sum_{j=1}^{3} \int_0^t \langle \alpha_s, e_j \rangle \, dX_s^j. \tag{2.22}$$

In the three states, the stock price process is governed by the geometric Brownian motion (GBM) (Black and Scholes, 1973), the Heston stochastic volatility model (Heston, 1993) and the double exponential Lévy model (Kou and Wang, 2004), respectively.

- *State 1: The stock price process follows the GBM model:*

$$dS_t^1 = S_t^1[r_1 dt + \sigma_1 dW_t], \tag{2.23}$$

where σ_1 is the stock price volatility and r_1 is the corresponding risk-free interest rate in this regime. The associated log-stock price process satisfies

$$dX_t^1 = \left(r_1 - \frac{1}{2}\sigma_1^2\right)dt + \sigma_1 dW_t. \tag{2.24}$$

The characteristic function is given by

$$\Phi^1(u;t,x) = \exp\left\{iux + g^1(u,t)\right\}, \tag{2.25}$$

where

$$g^1(u,t) = \left[\left(r_1 - \frac{\sigma_1^2}{2}\right)iu - \frac{\sigma_1^2 u^2}{2}\right](T-t). \tag{2.26}$$

- *State 2: The stock price process follows the Heston stochastic volatility model:*

$$dS_t^2 = S_t^2[r_2 dt + \sqrt{V_t}dW_t], \tag{2.27}$$

$$dV_t = \kappa(\theta - V_t)dt + \sqrt{V_t}\sigma_v\left[\rho dW_t + \sqrt{1-\rho^2}d\bar{W}_t\right], \tag{2.28}$$

where V_t is the instantaneous variance of the stock price and r_2 is the risk-free interest rate. In Equation (2.28), κ, θ and σ_v are the speed of mean reversion, long-run average and volatility of the variance process, respectively. The correlation between the Brownian motion increments is denoted here as ρ. The log-stock price process satisfies

$$dX_t^2 = \left(r_2 - \frac{1}{2}V_t\right)dt + \sqrt{V_t}dW_t. \tag{2.29}$$

The characteristic function (see Lord and Kahl (2010)) is given by

$$\Phi^2(u;t,x,v) = \exp\left\{iux + g^2(u,t) + D(u,t)v\right\}, \tag{2.30}$$

where

$$g^2(u,t) = iur_2\tau + C(u,t) \tag{2.31}$$

with

$$\begin{aligned}
&\tau = T - t,\\
&c(u) = \frac{\kappa - iu\rho\sigma_v + d(u)}{\kappa - iu\rho\sigma_v - d(u)}, \quad \bar{c}(u) = \frac{1}{c(u)},\\
&d(u) = \sqrt{(\kappa - iu\rho\sigma_v)^2 + \sigma_v^2(iu + u^2)},\\
&C(u,t) = \frac{\kappa\theta}{\sigma_v^2}\left[(\kappa - iu\rho\sigma_v + d(u))\tau - 2\log\left(\frac{1 - c(u)e^{d(u)\tau}}{1 - c(u)}\right)\right]
\end{aligned}$$

$$= \frac{\kappa\theta}{\sigma_v^2}\left[(\kappa - iu\rho\sigma_v + d(u))\tau - 2\log\left(\frac{\bar{c}(u) - e^{d(u)\tau}}{\bar{c}(u) - 1}\right)\right],$$

$$D(u,t) = \frac{\kappa - iu\rho\sigma_v - d(u)}{\sigma_v^2}\frac{1 - e^{-d(u)\tau}}{1 - e^{-d(u)\tau}/c(u)}$$

$$= \frac{\kappa - iu\rho\sigma_v - d(u)}{\sigma_v^2}\frac{1 - e^{-d(u)\tau}}{1 - \bar{c}(u)e^{-d(u)\tau}}.$$

- *State 3: The stock price process follows the double exponential model:*

$$dS_t^3 = S_{t-}^3\left[r_3 dt + \sigma_3 dW_t + \int_{\mathbb{R}_0}(e^{\xi(y)} - 1)\widetilde{N}_3(dt, dy)\right], \tag{2.32}$$

where σ_3 is the corresponding stock price volatility, r_3 is the risk-free interest rate, $\xi(z)$ is the jump ratio, and $\widetilde{N}_3(\cdot,\cdot)$ is the Poisson random measure with Lévy measure $\nu_3(\cdot)$ defined by

$$\nu_3(dy) = \lambda\left[p\eta_+ e^{-\eta_+ y}1_{\{y\geq 0\}} + (1-p)\eta_- e^{\eta_- y}1_{\{y<0\}}\right]dy, \quad \lambda > 0, p \in [0,1], \eta_+ > 1, \eta_- > 0, \tag{2.33}$$

The log-stock price satisfies

$$dX_t^3 = \mu_3 dt + \sigma_3 dW_t + \int_{\mathbb{R}_0}\xi(z)\widetilde{N}_3(dt, dy), \tag{2.34}$$

with

$$\mu_3 := r_3 - \frac{1}{2}\sigma_3^2 - \int_{\mathbb{R}_0}\left[e^{\xi(y)} - 1 - \xi(y)\right]\nu_3(dy). \tag{2.35}$$

The characteristic function is given by

$$\Phi^3(u;t,x) = \exp\left\{iux + g^3(u,t)\right\}, \tag{2.36}$$

where

$$g^3(u,t) = \left[\mu_3 iu - \frac{\sigma_3^2 u^2}{2} + \int_{\mathbb{R}_0}\left(e^{iu\xi(y)} - 1 - iu\xi(y)\right)\nu_3(dy)\right](T-t). \tag{2.37}$$

Next, we show how the above 3-state stock price model is embedded in our framework. The stochastic factor process ζ_t is constructed as follows

$$\zeta_t^1 = \zeta_t^3 = 0 \text{ and } \zeta_t^2 = V_t, \quad \forall t \in [0,T], \tag{2.38}$$

and

$$\zeta_t := \sum_{j=1}^{3}\langle\alpha_0, e_j\rangle\,\zeta_0^j + \sum_{j=1}^{3}\int_0^t\langle\alpha_s, e_j\rangle\,d\zeta_s^j \tag{2.39}$$

$$= \langle\alpha_0, e_2\rangle\,V_0 + \int_0^t\langle\alpha_s, e_2\rangle\,dV_s. \tag{2.40}$$

Clearly, the characteristic functions in the three states satisfy the structural assumption in Equation (2.9). Indeed,

$$\Phi^j(u;t,X_t^j) = \mathbb{E}^Q\left[e^{iuX_T^j}|X_t^j\right] = \exp\left\{iuX_t^j + g^j(u,t) + D(u,t)\zeta_t^j\right\}, \quad \text{for } j = 1,3, \tag{2.41}$$

and

$$\Phi^2(u;t,X_t^2,V_t)=\mathbb{E}^Q\left[e^{iuX_T^2}|X_t^2,V_t\right]=\exp\left\{iuX_t^2+g^2(u,t)+D(u,t)V_t\right\}. \tag{2.42}$$

Therefore, the discounted characteristic function of the 3-state stock price model can be expressed as

$$\widetilde{\Phi}_{X_T}(u;t,x,\zeta)=\mathbb{E}^Q\left[e^{-\int_t^T r_s ds+iuX_T}|X_t=x,\zeta_t=\zeta\right]=e^{iux+D(u,t)\zeta}\left\langle\alpha_t,\Psi(u,t)1_3\right\rangle, \tag{2.43}$$

where

$$\frac{d\Psi(u,t)}{dt}=\left[-Diag(G(u,t)+r)+A\right]\Psi(u,t),\quad \Psi(u,T)=I_3 \tag{2.44}$$

with

$$\begin{aligned}G(u,t)&=\begin{pmatrix}-\left[\left(r_1-\frac{\sigma_1^2}{2}\right)iu-\frac{\sigma_1^2u^2}{2}\right]\\ -iur_2-\frac{\kappa\theta}{\sigma_v^2}\left[(\kappa-iu\rho\sigma_v+d(u))+\frac{2c(u)d(u)e^{d(u)\tau}}{1-c(u)e^{d(u)\tau}}\right]\\ -\left[\mu_3iu-\frac{\sigma_3^2u^2}{2}+\int_{\mathbb{R}_0}\left(e^{iu\xi(y)}-1-iu\xi(y)\right)\nu_3(dy)\right]\end{pmatrix}\\ &=\begin{pmatrix}-\left[\left(r_1-\frac{\sigma_1^2}{2}\right)iu-\frac{\sigma_1^2u^2}{2}\right]\\ -iur_2-\frac{\kappa\theta}{\sigma_v^2}\left[(\kappa-iu\rho\sigma_v+d(u))+\frac{2d(u)e^{d(u)\tau}}{\bar{c}(u)-e^{d(u)\tau}}\right]\\ -\left[\mu_3iu-\frac{\sigma_3^2u^2}{2}+\int_{\mathbb{R}_0}\left(e^{iu\xi(y)}-1-iu\xi(y)\right)\nu_3(dy)\right]\end{pmatrix}.\end{aligned} \tag{2.45}$$

The generalised characteristic function is given by

$$\widehat{\Phi}_{X_T}(\mathbf{u},\mathbf{B};t,x,\zeta)=\mathbb{E}^Q\left[e^{-\int_t^T r_s ds+iu_TX_T}B_T|X_t=x,\zeta_t=\zeta\right]=\left\langle\exp\{A(T-t)\}\alpha_t,\widehat{\mathbf{\Psi}}(t,x,\zeta,\alpha_t)\right\rangle, \tag{2.46}$$

where

$$\widehat{\mathbf{\Psi}}(t,x,\zeta,\alpha_t)=\left(\widehat{\Psi}_1(t,x,\zeta,\alpha_t),\widehat{\Psi}_2(t,x,\zeta,\alpha_t),\widehat{\Psi}_3(t,x,\zeta,\alpha_t)\right)^\top \tag{2.47}$$

with

$$\widehat{\Psi}_j(t,x,\zeta,\alpha_t)=e^{iu_jx+D(u_j,t)\zeta}\left\langle\alpha_t,\Psi(u_j,t)1_3\right\rangle B_j. \tag{2.48}$$

In the second example, the stock price follows a regime-switching stochastic volatility model:

Example 2.2. *The log-stock price and the stochastic variance processes are given by*

$$X_t=X_0+\sum_{j=1}^n\int_0^t\left\langle\alpha_s,e_j\right\rangle dX_s^j, \tag{2.49}$$

$$V_t=V_0+\sum_{j=1}^n\int_0^t\left\langle\alpha_s,e_j\right\rangle dV_s^j, \tag{2.50}$$

where

$$dX_t^j=\left(r_j-\frac{1}{2}V_t^j\right)dt+\sqrt{V_t^j}dW_t, \tag{2.51}$$

$$dV_t^j = \kappa(\theta_j - V_t^j)dt + \sqrt{V_t^j}\sigma_v\big[\rho dW_t + \sqrt{1-\rho^2}d\bar{W}_t\big]. \tag{2.52}$$

Indeed, the stock price process is governed by the Heston model with regime-switching:

$$dS_t^j = S_t^j\left[r_j dt + \sqrt{V_t^j}dW_t\right], \quad j = 1, 2, \ldots, n. \tag{2.53}$$

Again, as presented in Lord and Kahl (2010), the characteristic function of X_T^j is given by

$$\Phi^j(u;t,x,\zeta) = \mathbb{E}^Q\big[e^{iuX_T^j}|X_t^j = x, V_t^j = \zeta\big] = \exp\big\{iux + g^j(u,t) + D(u,t)\zeta\big\}, \tag{2.54}$$

where

$$g^j(u,t) = iur_j\tau + C^j(u,t),$$

$$\begin{aligned} C^j(u,t) &= \frac{\kappa\theta_j}{\sigma_v^2}\left[(\kappa - iu\rho\sigma_v + d(u))\tau - 2\log\left(\frac{1-c(u)e^{d(u)\tau}}{1-c(u)}\right)\right] \\ &= \frac{\kappa\theta_j}{\sigma_v^2}\left[(\kappa - iu\rho\sigma_v + d(u))\tau - 2\log\left(\frac{\bar{c}(u)-e^{d(u)\tau}}{\bar{c}(u)-1}\right)\right], \end{aligned}$$

and $c(u)$, $\bar{c}(u)$, $d(u)$, $D(u,t)$ are as defined in Example 2.1.

Therefore, the discounted characteristic function of X_T is represented as

$$\widetilde{\Phi}_{X_T}(u;t,x,\zeta) = \mathbb{E}^Q\big[e^{-\int_t^T r_s ds + iuX_T}|X_t = x, V_t = \zeta\big] = e^{iux + D(u,t)\zeta}\left\langle \alpha_t, \Psi(u,t)1_n\right\rangle, \tag{2.55}$$

where

$$\frac{d\Psi(u,t)}{dt} = \big[-Diag(G(u,t) + r) + A\big]\Psi(u,t), \quad \Psi(u,T) = I_n \tag{2.56}$$

with

$$G(u,t) = \big(g_t^1(u,t), g_t^2(u,t), \ldots, g_t^n(u,t)\big)^\top, \tag{2.57}$$

and

$$g_t^j(u,t) = -iur_j - \frac{\kappa\theta_j}{\sigma_v^2}\left[(\kappa - iu\rho\sigma_v + d(u)) + \frac{2c(u)d(u)e^{d(u)\tau}}{1-c(u)e^{d(u)\tau}}\right]. \tag{2.58}$$

The generalised characteristic function is expressed as

$$\widehat{\Phi}_{X_T}(\mathbf{u},\mathbf{B};t,x,\zeta) = \left\langle \exp\{A(T-t)\}\alpha_t, \widehat{\mathbf{\Psi}}(t,x,\zeta,\alpha_t)\right\rangle, \tag{2.59}$$

where

$$\widehat{\mathbf{\Psi}}(t,x,\zeta,\alpha_t) = \big(\widehat{\Psi}_1(t,x,\zeta,\alpha_t), \widehat{\Psi}_2(t,x,\zeta,\alpha_t), \ldots, \widehat{\Psi}_n(t,x,\zeta,\alpha_t)\big)^\top \tag{2.60}$$

with

$$\widehat{\Psi}_j(t,x,\zeta,\alpha_t) = e^{iu_jx + D(u_j,t)\zeta}\left\langle \alpha_t, \Psi(u_j,t)1_n\right\rangle B_j. \tag{2.61}$$

Note we have assumed that v_0, σ_v, κ, and ρ are regime-independent. This assumption is needed to ensure that the characteristic function of X_T^j satisfies the form presented in Equation (2.9). This assumption is also imposed in literature such as in Elliott and Lian (2013).

In wrapping up this section, we recall the results in Proposition 2.1. In the GRS model, Equation (2.11) does not admit an analytical solution in general due to the time-dependence of the coefficients $G(u,t)$. One can refer to Examples 2.1 and 2.2 for details about this complexity. In comparison, the similar matrix-valued ODE in the CRS model does have the closed-form solution presented in Equation (2.12). The novelty of this paper is that under the structural assumption in Equation (2.9), we can link the characteristic function of X_T with those of X_T^j even if we have not specified the probability laws of X_T^j, for $j = 1, 2, \ldots, n$, in Proposition 2.1. Indeed, this provides us tremendous flexibility to incorporate many existing and new regime-switching models as special cases of our GRS model. See, for instance, the CRS model reviewed in Appendix A and studied in Elliott et al. (2005), and the regime-switching Heston model in Example 2.2 and considered in Elliott and Lian (2013). To our best knowledge, Example 2.1 is an entirely new regime-switching modelling setting, which allows for different model types in different states.

3 The Cosine method

In this section, we first provide a review of the ideas around the Fourier Cosine (COS) method for option pricing. The probability density function of any random variable X, denoted by $f_X(x)$, can be expressed in the cosine expansion as[1]

$$f_X(x) = \sum_{k=0}^{\infty}{}' A_X(k) \cdot \cos\left(k\pi \frac{x-a}{b-a}\right), \tag{3.1}$$

where $\sum'$ means that the first term of the sum is halved and

$$A_X(k) = \frac{2}{b-a}\int_a^b f_X(x) \cdot \cos\left(k\pi \frac{x-a}{b-a}\right) dx. \tag{3.2}$$

Note the characteristic function can be represented as a Fourier transform of the probability density function as

$$\widehat{\Phi}_X(u) = \int_a^b e^{iux} f_X(x) dx \approx \int_{-\infty}^{\infty} e^{iux} f_X(x) dx = \Phi(u). \tag{3.3}$$

Equation (3.2) can then be re-expressed as

$$\begin{aligned} A_X(k) &= \frac{2}{b-a} \cdot \mathrm{Re}\left\{\int_a^b f_X(x) \exp\left\{ik\pi \frac{x-a}{b-a}\right\} dx\right\} \\ &= \frac{2}{b-a} \cdot \mathrm{Re}\left\{\exp\left\{-\frac{ik\pi a}{b-a}\right\} \int_a^b \exp\left\{\frac{ik\pi}{b-a}x\right\} f_X(x) dx\right\} \\ &= \frac{2}{b-a} \cdot \mathrm{Re}\left\{\widehat{\Phi}_X\left(\frac{k\pi}{b-a}\right) \exp\left\{-\frac{ik\pi a}{b-a}\right\}\right\}. \end{aligned} \tag{3.4}$$

[1] See Fang and Oosterlee (2008), Alonso-García et al. (2018), and Tour et al. (2018), among others.

We can then write

$$F_X(k) = \frac{2}{b-a} \cdot \mathrm{Re}\left\{\Phi_X\left(\frac{k\pi}{b-a}\right)\exp\left\{-\frac{ik\pi a}{b-a}\right\}\right\}. \tag{3.5}$$

After truncating the summation, Equation (3.1) can then be approximated by

$$\widetilde{f}_X(x) = \sum_{k=0}^{N-1}{}' F_X(k) \cdot \cos\left(k\pi\frac{x-a}{b-a}\right). \tag{3.6}$$

To apply the COS method to the valuation of guaranteed minimum benefits (GMBs) under the GRS models, we consider first the valuation of a European style option with any payoff function $h(X_T)$, where X_T is the log-stock price at the maturity date. Then, the time-zero price of the option can be represented as

$$\begin{aligned} V(0,T,x_0,\alpha_0) &= \mathbb{E}^Q\left[e^{-\int_0^T r_t dt}h(X_T)\right] \\ &= \mathbb{E}^Q\left[e^{-\int_0^T r_t dt}\mathbb{E}^Q\left[h(X_T)|\mathcal{F}_T^\alpha\right]\right]. \end{aligned} \tag{3.7}$$

Here the second equality is due to the tower property.

Let $f_{X_T}(x|x_0)$ be the probability density function of $X_T = x$ given $X_0 = x_0$, and $f_{X_T}(x|x_0,\mathcal{F}_T^\alpha)$ be the (conditional) probability density function of $X_T = x$ given $X_0 = x_0$ and $\mathcal{F}_T^\alpha$. The option price can be represented by

$$V(0,T,x_0,\alpha_0) = \mathbb{E}^Q\left[e^{-\int_0^T r_t dt}\int_{-\infty}^{\infty} h(x) f_{X_T}(x|x_0,\mathcal{F}_T^\alpha)dx\right]. \tag{3.8}$$

As the density function mass is concentrated around the origin and zero everywhere (Fang and Oosterlee, 2008), we truncate the integration domain into the interval $[a_T, b_T]$ such that

$$V(0,T,x_0,\alpha_0) = \mathbb{E}^Q\left[e^{-\int_0^T r_t dt}\int_{a_T}^{b_T} h(x) f_{X_T}(x|x_0,\mathcal{F}_T^\alpha)dx\right], \tag{3.9}$$

where the lower and upper bounds a_T and b_T are dependent on the state of the chain at T, that is, α_T. By substituting the density function expansion presented in Equation (3.1), we obtain

$$\begin{aligned} V(0,T,x_0) &= \mathbb{E}^Q\left[e^{-\int_0^T r_t dt}\int_{a_T}^{b_T} h(x)\sum_{k=0}^{\infty}{}' A_{X_T}(k,x_0,\alpha_T,\mathcal{F}_T^\alpha)\cdot\cos\left(k\pi\frac{x-a_T}{b_T-a_T}\right)dx\right] \\ &= \mathbb{E}^Q\left[e^{-\int_0^T r_t dt}\int_{a_T}^{b_T} h(x)\sum_{k=0}^{N-1}{}' F_{X_T}(k,x_0,\alpha_T,\mathcal{F}_T^\alpha)\cdot\cos\left(k\pi\frac{x-a_T}{b_T-a_T}\right)dx\right] \\ &= \mathbb{E}^Q\left[e^{-\int_0^T r_t dt}\sum_{k=0}^{N-1}{}' F_{X_T}(k,x_0,\alpha_T,\mathcal{F}_T^\alpha)\int_{a_T}^{b_T} h(x)\cos\left(k\pi\frac{x-a_T}{b_T-a_T}\right)dx\right]. \end{aligned} \tag{3.10}$$

Here

$$F_{X_T}(k,x_0,\alpha_T,\mathcal{F}_T^\alpha) = \frac{2}{b_T-a_T}\cdot\mathrm{Re}\left\{\Phi_{X_T}\left(\frac{k\pi}{b_T-a_T};x_0,\mathcal{F}_T^\alpha\right)\exp\left\{-\frac{ik\pi a_T}{b_T-a_T}\right\}\right\}, \tag{3.11}$$

with

$$\Phi_{X_T}\left(\frac{k\pi}{b_T-a_T};x_0,\mathcal{F}_T^\alpha\right) = \mathbb{E}^Q\left[e^{i\cdot\frac{k\pi}{b_T-a_T}\cdot X_T}|\mathcal{F}_T^\alpha\right], \tag{3.12}$$

and $A_{X_T}(k, x_0, \alpha_T, \mathcal{F}_T^\alpha)$ can be defined similarly as $F_{X_T}(k, x_0, \alpha_T, \mathcal{F}_T^\alpha)$ (refer to Equations (3.2)-(3.5)) but with the domain of the integration in $\Phi_{X_T}(\frac{k\pi}{b_T - a_T}; x_0, \mathcal{F}_T^\alpha)$ truncated into $[a_T, b_T]$.

Letting

$$I_h(k, \alpha_T) = \int_{a_T}^{b_T} h(x) \cos\left(k\pi \frac{x - a_T}{b_T - a_T}\right) dx \tag{3.13}$$

and

$$\mathbf{c}(k) = (c_1(k), c_2(k), \ldots, c_n(k))^\top, \quad \mathbf{B}(k) = (B_1(k), B_2(k), \ldots, B_n(k))^\top, \tag{3.14}$$

with

$$c_j(k) = \frac{k\pi}{b_j - a_j}, \quad B_j(k) = \frac{2}{b_j - a_j} e^{-\frac{ik\pi a_j}{b_j - a_j}} I_h(k, \mathbf{e}_j), \tag{3.15}$$

the expectation in (3.10) can then be computed as

$$\begin{aligned} \mathbb{E}^Q\left[e^{-\int_0^T r_t dt} F_{X_T}(k, x_0, \alpha_T, \mathcal{F}_T^\alpha) I_h(k, \alpha_T)\right] &= \mathbb{E}^Q\left[e^{-\int_0^T r_t dt} \mathrm{Re}\left\{\Phi_{X_T}\left(\frac{k\pi}{b_T - a_T}; x_0, \mathcal{F}_T^\alpha\right) B_T(k)\right\}\right] \\ &= \mathrm{Re}\left\{\widehat{\Phi}_{X_T}\left(\mathbf{c}(k), \mathbf{B}(k); x_0\right)\right\}, \end{aligned} \tag{3.16}$$

where

$$\begin{aligned} \widehat{\Phi}_{X_T}\left(\mathbf{c}(k), \mathbf{B}(k); x_0\right) &= \mathbb{E}^Q\left[e^{-\int_0^T r_t dt} \Phi_{X_T}\left(\frac{k\pi}{b_T - a_T}; x_0, \mathcal{F}_T^\alpha\right) B_T(k)\right] \\ &= \mathbb{E}^Q\left[e^{-\int_0^T r_t dt + i \cdot \frac{k\pi}{b_T - a_T} \cdot X_T} B_T(k)\right]. \end{aligned} \tag{3.17}$$

Therefore, using the COS method, we can approximate the option price by

$$V(0, T, x_0) = \sum_{k=0}^{N-1}{}' \mathrm{Re}\left\{\widehat{\Phi}_{X_T}\left(\mathbf{c}(k), \mathbf{B}(k); x_0\right)\right\}. \tag{3.18}$$

4 Guaranteed minimum maturity benefits valuation

In this section, we present three typical payoff functions of guaranteed minimum maturity benefits embedded in variable annuity contract. We derive explicit valuation expressions for the respective payoffs. The payoff of a guaranteed minimum maturity benefit (GMMB) can be represented as

$$\vartheta(S_T, G_T) = \max\{S_T, G_T\}, \tag{4.1}$$

where[2]

$$G_T = \begin{cases} G & \text{if the guarantee is fixed,} \\ Ge^{\delta T} & \text{if the guarantee is rolled up at a rate of } \delta, \\ \left(\prod_{m=0}^T S_m\right)^{\frac{1}{T+1}} & \text{if it is a ratchet geometric average guarantee.} \end{cases} \tag{4.2}$$

[2]For the ratchet features we consider the floating strike case which is one of the most less trivial cases.

The valuation of the fixed and roll-up cases can be accomplished uniformly as detailed below, where for convenience, G_T is either equal to G or $Ge^{\delta T}$.

Subsection 4.1 presents the fixed and roll-up guarantee cases. Note that the fixed guarantee is a special case of the roll-up case. We then derive valuation expressions for the geometric average guarantee case which is more complex in Subsection 4.2.

4.1 Fixed and roll-up cases

The payoff of a GMMB can be represented as

$$\begin{aligned}\vartheta(S_T, G_T) = \max\{S_T, G_T\} &= S_T + \max\{G_T - S_T, 0\} \\ &= G_T + \max\{S_T - G_T, 0\},\end{aligned} \tag{4.3}$$

where S_T and G_T are the underlying investment fund value/stock price and the minimum guarantee at maturity, respectively. The two decompositions in Equation (4.3) are equivalent and will lead to the same VA contract prices as long as taxation rules are not incorporated. When taxes are factored, price differences may occur depending on the jurisdiction (see Alonso-García et al. (2020) and Moenig and Bauer (2016) for detailed discussions incorporating taxation). The first decomposition is usually presented from the provider's perspective, while the second equality is more naturally associated with the policyholder's perspective. In the fixed and roll-up cases, we use the second equality for all derivations. Whereas, in the ratchet geometric average case we adopt a decomposition (refer to (4.21)) equivalent to the first equality in Equation (4.3).

Recalling the log-stock price defined as $X_t := \log(S_t)$, for any $t \in [0, T]$, particularly the initial log-stock price as $x_0 := \log S_0$, we have $S_T = e^{X_T}$. Letting $h_M(x) := \max\{e^x - G_T, 0\}$, the value of a GMMB rider can be calculated as

$$\begin{aligned}V_M(0, T, x_0) &= \mathbb{E}^Q\left[e^{-\int_0^T r_t dt} G_T\right] + \mathbb{E}^Q\left[e^{-\int_0^T r_t dt} h(X_T)\right] \\ &= \left\langle \alpha_0, \exp\left\{[-\text{Diag}(r) + A]T\right\} 1_n \right\rangle G_T + \mathbb{E}^Q\left[e^{-\int_0^T r_t dt} h_M(X_T)\right],\end{aligned} \tag{4.4}$$

where the first term can be derived similarly as in the proof of Proposition 2.1. Substituting Equation (3.10) into the second component of (4.4) yields

$$V_M(0, T, x_0) = \left\langle \alpha_0, \exp\left\{[-\text{Diag}(r) + A]T\right\} 1_n \right\rangle G_T + {\sum_{k=0}^{N-1}}' \text{Re}\left\{\widehat{\Phi}_{X_T}\left(\mathbf{c}(k), \mathbf{B}(k); x_0\right)\right\}, \tag{4.5}$$

where $\mathbf{c}(k) = (c_1(k), c_2(k), \ldots, c_n(k))^\top$ and $\mathbf{B}(k) = (B_1(k), B_2(k), \ldots, B_n(k))^\top$ with

$$c_j(k) = \frac{k\pi}{b_j - a_j} \quad \text{and} \quad B_j(k) = \frac{2}{b_j - a_j} e^{-\frac{ik\pi a_j}{b_j - a_j}} I_M(k, \mathbf{e}_j). \tag{4.6}$$

Note that in Equation (4.5), $I_M(k, \mathbf{e}_j)$ are integral terms, for $k = 0, 1, \ldots, N-1$ and $j = 0, 1, \ldots, n$, that is

$$\begin{aligned}I_M(k, \mathbf{e}_j) &= \int_{a_j}^{b_j} \max\{e^x - G_T, 0\} \cos\left(k\pi \frac{x - a_j}{b_j - a_j}\right) dx \\ &= \int_{\ln G_T}^{b_j} (e^x - G_T) \cos\left(k\pi \frac{x - a_j}{b_j - a_j}\right) dx,\end{aligned} \tag{4.7}$$

which simplifies to[3]

$$\begin{aligned} I_M(k,\mathbf{e}_j) &= \int_{\ln G_T}^{b_j} e^x \cos\left(k\pi\frac{x-a_j}{b_j-a_j}\right)dx - G_T\int_{\ln G_T}^{b_j}\cos\left(k\pi\frac{x-a_j}{b_j-a_j}\right)dx \\ &= G_T\frac{b_j-a_j}{k\pi}\sin\left(k\pi\frac{\ln G_T-a_j}{b_j-a_j}\right) + \frac{\sin(k\pi)}{k\pi} + \frac{e^{b_j}}{1+\left(\frac{k\pi}{b_j-a_j}\right)^2}\left[\cos(k\pi)+\frac{k\pi}{b_j-a_j}\sin(k\pi)\right] \\ &\quad - \frac{G_T}{1+\left(\frac{k\pi}{b_j-a_j}\right)^2}\left[\cos\left(k\pi\frac{\ln G_T-a_j}{b_j-a_j}\right)+\frac{k\pi}{b_j-a_j}\sin\left(k\pi\frac{\ln G_T-a_j}{b_j-a_j}\right)\right], \quad \text{if } k\neq 0; \end{aligned} \tag{4.8}$$

and

$$I_M(k,\mathbf{e}_j) = e^{b_j} + G_T\left[\ln G_T - (b_j+1)\right], \quad \text{if } k=0. \tag{4.9}$$

Remark 4.1. *It remains to input the generalised characteristic function* $\widehat{\Phi}_{X_T}(\mathbf{c}(k),\mathbf{B}(k);x_0)$ *into Equation* (4.5)*. For the GRS model, the generalised characteristic functions in Examples 2.1 and 2.2 are given by Equations* (2.46) *and* (2.59)*, respectively.*

For the CRS model (see Appendix A), we next provide a detailed pricing formula as an illustration. Recall the price we aim to find is

$$V_M(0,T,x_0) = \left\langle \alpha_0, \exp\left\{[-Diag(r)+A]T\right\}1_n\right\rangle G_T + {\sum_{k=0}^{N-1}}' Re\left\{\widehat{\Phi}_{X_T}(\mathbf{c}(k),\mathbf{B}(k);x_0)\right\}. \tag{4.10}$$

In the CRS model, the generalised characteristic function evaluated at time 0 *has been presented in Equation* (A.10)*, that is*

$$\widehat{\Phi}_{X_T}(\mathbf{c}(k),\mathbf{B}(k);x_0) = \left\langle \exp\{AT\}\alpha_0, \widehat{\mathbf{\Psi}}(0,x_0,\alpha_0)\right\rangle, \tag{4.11}$$

where

$$\widehat{\mathbf{\Psi}}(0,x_0,\alpha_0) = \left(\widehat{\Psi}_1(0,x_0,\alpha_0),\widehat{\Psi}_2(0,x_0,\alpha_0),\ldots,\widehat{\Psi}_n(0,x_0,\alpha_0)\right)^\top \tag{4.12}$$

with

$$\widehat{\Psi}_j(0,x_0,\alpha_0) = e^{ic_j(k)x_0}\left\langle \alpha_0, \exp\left\{[-Diag(G(c_j(k))+r)+A]T\right\}1_n\right\rangle B_j(k), \tag{4.13}$$

$$c_j(k) = \frac{k\pi}{b_j-a_j}, \quad B_j(k) = \frac{2}{b_j-a_j}e^{-\frac{ik\pi a_j}{b_j-a_j}}I_M(k,\mathbf{e}_j), \tag{4.14}$$

and

$$G_j(u) := -\left\{iu\mu_j - \frac{1}{2}u^2\sigma_j^2 + \int_{\mathbb{R}_0}\left(e^{iu\xi_j(x)}-1-iu\xi_j(x)\right)\nu_j(dx)\right\}.$$

[3]Here, we make use of the identity

$$\int e^{mx}\cos(nx)dx = \frac{e^{mx}}{m^2+n^2}[n\sin(nx)+m\cos(nx)] + const.$$

Remark 4.2. *In the above analysis, we do not consider the management fees charged by the VA provider. In literature, it is usually assumed that a continuously compounded insurance fee is levied by the provider on the fund value. Let F_t be the time-t fee-adjusted fund value defined by $F_t = e^{-qt}S_t$, where q is the continuously compounded rate of insurance fee. When the fee is taken into account, everything else being identical, the payoff of a GMMB becomes*[4]

$$\begin{aligned}\vartheta(F_T, G_T) &= \max\{F_T, G_T\} = \max\{e^{-qT}S_T, G_T\} \\ &= e^{-qT}\max\{S_T, e^{qT}G_T\} = e^{-qT}\max\{S_T, \bar{G}_T\},\end{aligned} \tag{4.15}$$

where

$$\bar{G}_T = \begin{cases} Ge^{qT} & \text{if the guarantee is fixed,} \\ Ge^{(\delta+q)T} & \text{if the guarantee is rolled up at a rate of } \delta. \end{cases} \tag{4.16}$$

Therefore, both the fixed and rolled up guarantees can be tackled under the original rolled up case in Equation (4.2)*, with rates q and $\delta + q$, respectively. We can adapt all the results derived in this subsection to the case with the continuously compounded rate of insurance fee q, if we scale Equation* (4.4) *by e^{-qT} and simultaneously replace G_T by $\bar{G}_T$ in Equation* (4.4)*.*

Remark 4.3. *The Greeks for the GMMB rider can be computed using standard manipulations (see Remark 3.2 in Fang and Oosterlee (2008) for details) as follows:*

$$\Delta = \frac{1}{S_0}\sum_{k=0}^{N-1}{}' Re\left\{\widehat{\Phi}_{X_T}\left(\mathbf{c}(k), \mathbf{B}^{\Delta}(k); x_0\right)\right\}, \tag{4.17}$$

where $\mathbf{B}^{\Delta}(k) := (B_1^{\Delta}(k), B_2^{\Delta}(k), \ldots, B_n^{\Delta}(k))^{\top}$ with

$$B_j^{\Delta}(k) := B_j(k)\cdot\frac{ik\pi}{b_j - a_j} = \frac{2ik\pi}{(b_j - a_j)^2}e^{-\frac{ik\pi a_j}{b_j - a_j}}I_M(k, \mathbf{e}_j). \tag{4.18}$$

The gamma can also be shown to be

$$\Gamma = \frac{1}{S_0^2}\sum_{k=0}^{N-1}{}' Re\left\{\widehat{\Phi}_{X_T}\left(\mathbf{c}(k), \mathbf{B}^{\Gamma}(k); x_0\right)\right\}, \tag{4.19}$$

where $\mathbf{B}^{\Gamma}(k) := (B_1^{\Gamma}(k), B_2^{\Gamma}(k), \ldots, B_n^{\Gamma}(k))^{\top}$ with

$$B_j^{\Gamma}(k) := \left(-\frac{ik\pi}{b_j - a_j} + \left(\frac{ik\pi}{b_j - a_j}\right)^2\right)\cdot B_j(k) = \left(-\frac{ik\pi}{b_j - a_j} + \left(\frac{ik\pi}{b_j - a_j}\right)^2\right)\frac{2}{b_j - a_j}e^{-\frac{ik\pi a_j}{b_j - a_j}}I_M(k, \mathbf{e}_j). \tag{4.20}$$

4.2 GMMB with the ratchet floating strike geometric average feature

The payoff of a GMMB with ratchet features can be represented as

$$\vartheta(S_T, G_T) = \max\left\{\left(\prod_{m=0}^{T} S_m\right)^{\frac{1}{T+1}}, S_T\right\}$$

[4]Analysis of the impact of fees is usually performed on contracts where the policyholder has the option to surrender early, see Kang and Ziveyi (2018) for details.

$$= S_T + \max\left\{\left(\prod_{m=0}^{T} S_m\right)^{\frac{1}{T+1}} - S_T, 0\right\}$$
$$= S_T + \max\{G_T - S_T, 0\}, \tag{4.21}$$

where $G_T = \left(\prod_{m=0}^{T} S_m\right)^{\frac{1}{T+1}}$. Denoting the second term in the last equality of Equation (4.21) as

$$h_R(S_T) \equiv \max\{G_T - S_T, 0\}, \tag{4.22}$$

the value of the ratchet option can be represented as

$$\begin{aligned}\tilde{V}_R(0,T,x_0) &= \mathbb{E}^Q\left[e^{-\int_0^T r_t dt} h_R(S_T)\right] \\ &= \mathbb{E}^Q\left[e^{-\int_0^T r_t dt} \max\{G_T - S_T, 0\}\right] \\ &= \mathbb{E}^Q\left[e^{-\int_0^T r_t dt} S_T \max\left\{\frac{G_T}{S_T} - 1, 0\right\}\right]. \end{aligned} \tag{4.23}$$

The above equation can be expressed as

$$\tilde{V}_R(0,T,x_0) = S_0\mathbb{E}^Q\left[e^{-\int_0^T r_t dt}\frac{S_T}{S_0} \max\left\{\frac{G_T}{S_T} - 1, 0\right\}\right]. \tag{4.24}$$

Since the discounted stock price process is a Q-martingale, we can change the probability measure by letting

$$\left.\frac{d\tilde{Q}}{dQ}\right|_{\mathcal{F}_T} = \eta_T = e^{-\int_0^T r_t dt}\frac{S_T}{S_0}. \tag{4.25}$$

Equation (4.24) is then equivalent to

$$\tilde{V}_R(0,T,x_0) = S_0\mathbb{E}^{\tilde{Q}}\left[\max\left\{\frac{G_T}{S_T} - 1, 0\right\}\right]. \tag{4.26}$$

where $\mathbb{E}^{\tilde{Q}}[\cdot]$ denotes the expectation taken under $\tilde{Q}$.

To calculate the above equation, we first let[5] $Z_m = \ln(G_m/S_m)$, for any $m = 0, 1, \cdots, T$, and denote by $f_{Z_T}(z|\mathcal{F}_T^\alpha, z_0)$ the probability density function of Z_T under $\tilde{Q}$ given $Z_0 = z_0$. Note that $Z_0 = z_0 = \ln(G_0/S_0) = 0$. Thus we suppress the dependence of the density function on the initial value z_0 and write $f_{Z_T}(z|\mathcal{F}_T^\alpha) := f_{Z_T}(z|\mathcal{F}_T^\alpha, z_0)$. Therefore, we can express Equation (4.26) as

$$\begin{aligned}\tilde{V}_R(0,T,x_0) &= S_0\mathbb{E}^{\tilde{Q}}\left[\max\left\{e^{Z_T} - 1, 0\right\}\right] \\ &= S_0\mathbb{E}^{\tilde{Q}}\left[\int_{-\infty}^{\infty} \max\left\{e^z - 1, 0\right\} f_{Z_T}(z|\mathcal{F}_T^\alpha)dz\right] \\ &\approx S_0\mathbb{E}^{\tilde{Q}}\left[\int_{a_T}^{b_T} \max\left\{e^z - 1, 0\right\} f_{Z_T}(z|\mathcal{F}_T^\alpha)dz\right] \\ &= S_0 \sum_{k=0}^{N-1}{}' \mathrm{Re}\left\{\widehat{\Phi}_{Z_T}\left(\mathbf{c}(k), \mathbf{H}(k)\right)\right\}, \end{aligned} \tag{4.27}$$

where $\mathbf{c}(k) = (c_1(k), c_2(k), \cdots, c_n(k))^\top$ and $\mathbf{H}(k) = (H_1(k), H_2(k), \cdots, H_n(k))^\top$ with

$$c_j(k) = \frac{k\pi}{b_j - a_j}, \quad H_j(k) = \frac{2}{b_j - a_j} e^{-\frac{ik\pi a_j}{b_j - a_j}} I_R(k, \mathbf{e}_j) \tag{4.28}$$

[5]Refer to Appendice B.3 and B.4 for derivations of the characteristic functions of Z_T.

and

$$
\begin{aligned}
I_R(k,\mathbf{e}_j) &= \int_{a_j}^{b_j} \max\{e^z-1,0\}\cos\left(k\pi\frac{z-a_j}{b_j-a_j}\right)dz \\
&= \int_0^{b_j} e^z\cos\left(k\pi\frac{z-a_j}{b_j-a_j}\right)dz - \int_0^{b_j}\cos\left(k\pi\frac{z-a_j}{b_j-a_j}\right)dz \\
&= -\frac{b_j-a_j}{k\pi}\sin\left(k\pi\frac{a_j}{b_j-a_j}\right) + \frac{\sin(k\pi)}{k\pi} + \frac{e^{b_j}}{1+\left(\frac{k\pi}{b_j-a_j}\right)^2}\left[\cos(k\pi)+\frac{k\pi}{b_j-a_j}\sin(k\pi)\right] \\
&\quad -\frac{1}{1+\left(\frac{k\pi}{b_j-a_j}\right)^2}\left[\cos\left(k\pi\frac{a_j}{b_j-a_j}\right)-\frac{k\pi}{b_j-a_j}\sin\left(k\pi\frac{a_j}{b_j-a_j}\right)\right], \quad \text{if } k\neq 0;
\end{aligned} \tag{4.29}
$$

and

$$
I_R(k,\mathbf{e}_j) = e^{b_j}-(b_j+1), \quad \text{if } k=0. \tag{4.30}
$$

Remark 4.4. *It remains to derive the function $\widehat{\Phi}_{Z_T}(\cdot)$. The derivations for the CRS model can be found in Appendix B.3. For the GRS model, $\widehat{\Phi}_{Z_T}(\cdot)$ should be derived case by case. Since the derivations for Examples 2.1 and 2.2 are equivalent, we only consider Example 2.2 and relegate the lengthy derivations of the corresponding $\widehat{\Phi}_{Z_T}(\cdot)$ to Appendix B.4.*

Therefore, substituting $\widehat{\Phi}_{Z_T}(\cdot)$ into Equation (4.27) and using (4.21), we obtain the value of a GMMB with ratchet features as

$$
\begin{aligned}
V_R(0,T,x_0) &= \mathbb{E}^Q\left[e^{-\int_0^T r_t dt}\vartheta(S_T,G_T)\right] \\
&= \mathbb{E}^Q\left[e^{-\int_0^T r_t dt}S_T\right] + \tilde{V}_R(0,T,x_0) \\
&= S_0\left[1+{\sum_{k=0}^{N-1}}'\mathrm{Re}\left\{\widehat{\Phi}_{Z_T}\left(\mathbf{c}(k),\mathbf{H}(k)\right)\right\}\right].
\end{aligned} \tag{4.31}
$$

One can refer to Equations (B.25) and (B.58) for the explicit expressions for the CRS model and Example 2.2, respectively.

Remark 4.5. *Similarly, when guarantee fees are taken into account, everything else being identical, the payoff of a GMMB becomes*

$$
\vartheta(F_T,G_T) = \max\left\{\left(\prod_{m=0}^{T}F_m\right)^{\frac{1}{T+1}},F_T\right\}, \tag{4.32}
$$

where the dynamics of $F_t = e^{-qt}S_t$ satisfies

$$
\frac{dF_t}{F_t} = (r_t-q)dt+\cdots, \quad t\in[0,T], \quad F_0=S_0,
$$

with "$\cdots$" representing omitted Q-martingale components. Recall that the stock price process evolves as

$$
\frac{dS_t}{S_t} = r_t dt+\cdots, \quad t\in[0,T].
$$

Therefore, we can adapt all the results derived in this subsection to the case with the continuously compounded rate of insurance fee q, if we scale Equation (4.31) *by e^{-qT} and simultaneously replace the risk-free interest rate from r_t by $r_t - q$. That is,*

$$\begin{aligned} V_R(0,T,x_0) &= \mathbb{E}^Q\left[e^{-\int_0^T r_t dt}\vartheta(F_T,G_T)\right] \\ &= e^{-qT}\mathbb{E}^Q\left[e^{-\int_0^T (r_t-q)dt}\vartheta(F_T,G_T)\right]. \end{aligned}$$

5 Numerical illustrations

In this section, we perform extensive numerical experiments showcasing the computational efficiency of the COS method in terms of speed and accuracy under the settings presented in Section 4 above. All efficiency tests are assessed relative to the Monte Carlo simulation. In enhancing the accuracy of the COS method, this paper makes a unique contribution by devising an algorithm for optimally selecting the number of grid points, N, such that the computed variable annuity contract values are within a given error tolerance. Prior literature has predominantly chosen the grid points to be 2^N, with N being a positive integer. This paper shows that this does not necessarily need to be the case. Instead, we derive an explicit relationship between the number of grid points and approximation error for the COS method. This section is organised into two parts. Subsection 5.1 contains all numerical experiments relating to the fixed and roll-up guarantees considered in Subsection 4.1. Subsection 5.2 is exclusive for numerical analysis for the ratchet guarantee case presented in Subsection 4.2. Subsections 5.1 and 5.2 are based on Examples 2.1 and 2.2, respectively. Recall that pricing formulas for the ratchet guarantee case should be derived case by case and we only provide the derivations for the CRS model and Example 2.2 in Appendices B.3-B.4. Though we can easily adapt those derivations to Example 2.1, they are very lengthy and involve no further innovations. Indeed, even the pricing formula itself for Example 2.1 would be fairly lengthy in the ratchet guarantee case. For this reason, we prefer neither to derive the pricing formula for Example 2.1 nor to provide the pricing formula without derivations for Example 2.1. This is also the reason why we focus on the two different examples in Subsections 5.1 and 5.2, respectively. The purpose of numerical illustrations is to demonstrate the generality and efficiency of our framework to accommodate a wide range of models. Since the underlying models in Examples 2.1-2.2 and the payoff functions in the fixed/roll-up and rachet cases are quite different, we do not need to compare the VA contract prices across examples or payoff functions.

5.1 Variable annuity embedded with fixed GMMB

In this subsection, we exclusively present convergence tests and sensitivity analysis for the variable annuity when the guarantee is fixed. The general findings hold for the roll-up guarantee case, as such we consider the following payoff at maturity

$$\vartheta(S_T,G) = \max(S_T,G).$$

For all numerical illustrations in this subsection, unless otherwise stated, we use the parameter set presented in Table 1. Efficiency tests of the COS method relative to the Monte Carlo approach in terms of computational speed and convergence analysis are presented in Subsection 5.1.1. Sensitivity tests relating to changes in variable annuity contract prices relative to underlying state variables are presented in Subsection 5.1.2.

Regime	GBM	Heston	Double Exponential
	$r_1 = 0.01$	$r_2 = 0.02$	$r_3 = 0.01$
	$\sigma_1 = 0.2$	$\sigma_v = 0.01$	$\sigma_3 = 0.2$
		$\theta = 0.04$	$\lambda = 0.35$
		$\kappa = 10$	$p = 0.8$
			$\eta_+ = 30$, $\eta_- = 50$

Table 1: Parameter set for all numerical experiments performed for the fixed and roll-up cases. Unless otherwise stated, we assume that the initial stock price/underlying fund value is $S_0 = 0.9$, the initial guarantee $G = 1$ and maturity $T = 30$.

5.1.1 Computational efficiency analysis

For all analysis in this subsection, we compare the performance of our proposed COS method against the Monte Carlo simulation. In particular, we stop the computation of the COS method when the marginal incremental value has an absolute error below $1e-5$. In so doing, we optimally choose the grid size, N, of the COS method such that the resulting error is less than $1e-5$. We take the price computed with $N = 2^9$ grid-points in the COS method as the pseudo true value to benchmark the results. In what follows, we will report the following:

- the time in seconds, T_{cos} and the grid size, N of the proposed COS method;
- the time in seconds, T_{mc} and the number of Monte-Carlo sample, M such that the resulting Monte-Carlo estimate is less than $5e-3$ to the pseudo true value and with standard error less than $5e-3$.

Note that we have ignored the Monte Carlo bias in the scheme, which exists when conditional density is not analytically available. Instead, we rely on the Euler scheme to approximate the conditional density of the underlying stochastic processes. For all numerical illustrations that follow, we set the time steps $dt = 1e-3$ for sampling the Euler scheme, which ensures a negligible approximation bias. Below we perform successive analysis for three settings. The single-regime case is equivalent to the standard case without regime-switching, where the underlying fund dynamics follows either the GBM model, Heston stochastic volatility model or the double exponential (DE) model. The second is the two-regime case which is a combination of any two of the models. The third case involves all the three regimes under consideration.

Single-regime cases

We first consider the single-regime cases. Table 2 presents efficiency comparisons between the COS method and Monte Carlo simulation. Among the three models, the Heston stochastic volatility model requires substantial computational costs for the Monte Carlo method to approximate the corresponding stochastic differential equation as reflected in Table 2. It takes a fraction of a second for the COS method to generate accurate VA prices across all scenarios presented. We also note that for the Heston stochastic volatility case, more grid points are required for the COS method relative to either the GBM model or the DE model to achieve accuracy within the error tolerance of $1e-5$. In summary, the Monte Carlo method is particularly efficient for a single regime where the step-wise conditional density is known and easy to sample. This is the case for the GBM and DE models.

	COS			Monte Carlo		
	Price	N	T_{cos}	Price	M	T_{mc}
GBM	1.1656	53	0.2163	1.1657	63,960	0.1414
Heston	1.0507	152	0.8739	1.0506	68,518	136.5889
DE	1.1665	53	0.2443	1.1640	67,685	0.1584

Table 2: Comparison of the COS method and Monte Carlo approach in the single-regime cases. All other parameters are as presented in Table 1 above.

Two-regime cases

When there is more than one regime, sampling of the Markov transition is relatively extensive. One approach considers the sampling of inter-jump times as exponential random variables and evolves the state between the jump times depending on the current regime. Alternatively, we can also consider an Euler scheme such that we approximate the continuous state transition according to the discrete case with the transition probability matrix denoted as

$$P = \exp(Adt),$$

with dt being an instantaneous time (Yuan and Mao, 2004). Here, we assume that $dt = 1e-3$ similar to the Heston stochastic volatility case described above. We analyse three scenarios of the two-regime cases, where the transition rate matrices are presented as

$$A_1 = \begin{pmatrix} -0.5 & 0 & 0.5 \\ 0 & 0 & 0 \\ 0.5 & 0 & -0.5 \end{pmatrix}, \quad A_2 = \begin{pmatrix} -0.5 & 0.5 & 0 \\ 0.5 & -0.5 & 0 \\ 0.0 & 0 & 0.0 \end{pmatrix}, \quad A_3 = \begin{pmatrix} 0.0 & 0.0 & 0.0 \\ 0 & -0.5 & 0.5 \\ 0.0 & 0.5 & -0.5 \end{pmatrix},$$

where the initial regime can either be GBM or DE model, GBM or Heston model, Heston or DE model in the three scenarios, respectively. Table 3 shows price comparisons and the corresponding computational costs of

the two methods. The computational cost of the COS method is very low (less than a second) irrespective of the initial regime relative to Monte Carlo simulation which elapses at least 126 seconds to generate comparable prices.

	COS			Monte Carlo		
	Price	N	T_{cos}	Price	M	T_{mc}
A_1, GBM	1.1672	53	0.3041	1.1658	57,344	126.1446
A_1, DE	1.1672	53	0.4427	1.1622	63,428	265.9906
A_2, GBM	1.1048	64	0.3799	1.1007	63,181	145.9834
A_2, Heston	1.1019	170	0.8514	1.1024	64,476	150.0725
A_3, Heston	1.1016	71	0.5494	1.1028	63,930	203.5537
A_3, DE	1.1050	71	0.3666	1.1083	67,049	216.0365

Table 3: Comparison of the COS method and Monte Carlo approach in the two-regime cases. All other parameters are as presented in Table 1.

Three-regime cases

We now consider computational efficiency of the three-regime cases and perform our numerical illustrations by assuming the following transition rate matrix

$$A = \begin{pmatrix} -0.6 & 0.3 & 0.3 \\ 0.3 & -0.6 & 0.3 \\ 0.3 & 0.3 & -0.6 \end{pmatrix} \tag{5.1}$$

with the regimes ordered as the GBM, Heston, and DE models, respectively. Consistent with the two-regime cases, we note the superiority of the COS method in terms of computational efficiency as reflected in Table 4. From this table, we note a slight increase in the number of grid points is required to achieve the target accuracy level for the COS method. However, the corresponding computational cost does not increase substantially compared to the single-regime and two-regime cases.

	COS			Monte Carlo		
	Price	N	T_{cos}	Price	M	T_{mc}
GBM	1.1676	95	0.6605	1.1659	64,926	199.4552
Heston	1.1641	108	0.8689	1.1604	62,662	192.9726
DE	1.1676	95	0.4831	1.1646	64,276	197.3541

Table 4: Comparison of the COS method and Monte Carlo approach in the three-regime cases. All other parameters are as presented in Table 1.

To highlight this point, we perform convergence analysis for the COS method in Figure 1. In this figure,

we present the convergence of the COS method in the scenario where the initial state is the GBM. To check the rate of convergence, we obtain approximations with a grid for larger values of N, and plot the negative logarithm of the absolute difference between the approximated and true values against $\log(N)$. Note that in theory $\epsilon \approx N^{-\alpha}$ for N large, where ϵ is the absolute value of the approximation error. This implies that

$$-\log(|\epsilon|) = \alpha \log(N) + c,$$

as plotted on the right panel of Figure 1, where c is some constant independent of N. From the left plot of Figure 1, strong convergence is achieved for $N < 100$ implying low computational cost associated with the COS method for higher levels of accuracy.

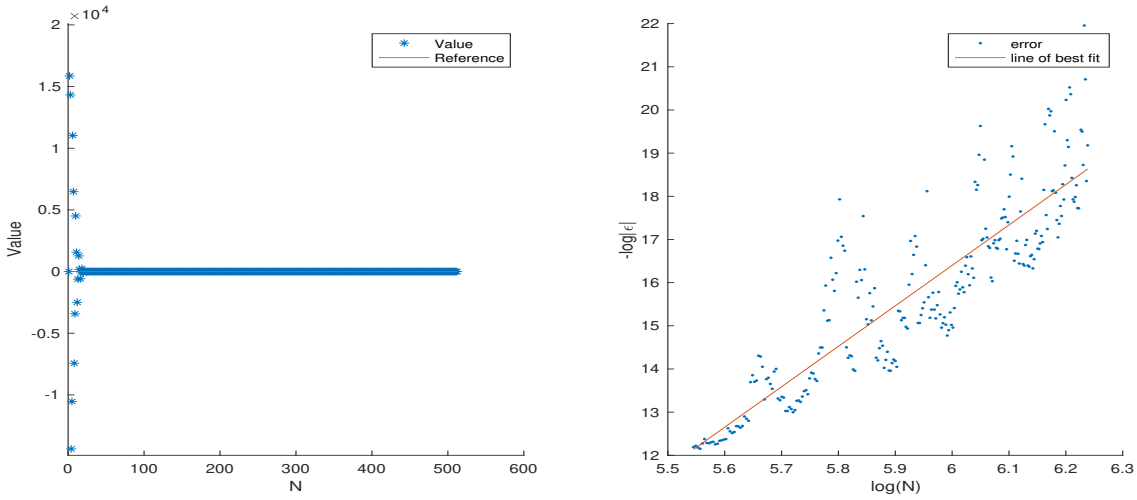

Figure 1: Convergence plots of the COS method. The line of best fit for $-\log(|\epsilon|)$ against $\log(N)$ is $-\log(|\epsilon|) = -39.7064 + 9.3684 \log(N)$. The reference is taken from the value computed via the COS method using $N = 2^{11}$. All other parameters are as presented in Table 1.

5.1.2 Sensitivity analysis under the three-regime framework

Having presented convergence tests for the GMMB with fixed guarantee in the above subsection, we now perform sensitivity analysis to investigate the behaviour of the variable annuity contract with respect to changes in the underlying state variables. Figure 2 contains subplots of the changes in variable annuity prices with respect to changes in the guarantee level (G), initial fund value (S_0), and maturity of the contract (T), respectively. In this analysis, we have assumed the GBM to be the initial state with all other parameters as presented in Table 1.

From Figure 2, we note that the VA price is an increasing function of both the guarantee and underlying fund value which is in line with increasing risk from the VA provider's perspective. A humped sensitivity with respect to the contract maturity is also evident in all our numerical illustrations, with the peak around $T = 23$. We have tested the results with other initial states, and the general conclusion is consistent. This behaviour is

consistent with existing literature on GMMB riders which note the concavity of prices with respect to maturity (Bernard et al., 2014; Kang and Ziveyi, 2018). This is because a (European) call option and a constant payment are embedded in the fixed guarantee rider, as shown in the first decomposition of Equation (4.3). The call option price increases with the time-to-maturity, and the actuarial present value of the constant payment decreases with the time-to-maturity. The combined effect is reflected by the concave relationship between the VA price and the time-to-maturity. For completeness, we also provide a surface plot highlighting the behaviour of the VA contract prices to changes in the initial fund value and time-to-maturity when the initial state is the GBM in Figure 3. We note consistent behaviour as highlighted in Figure 2.

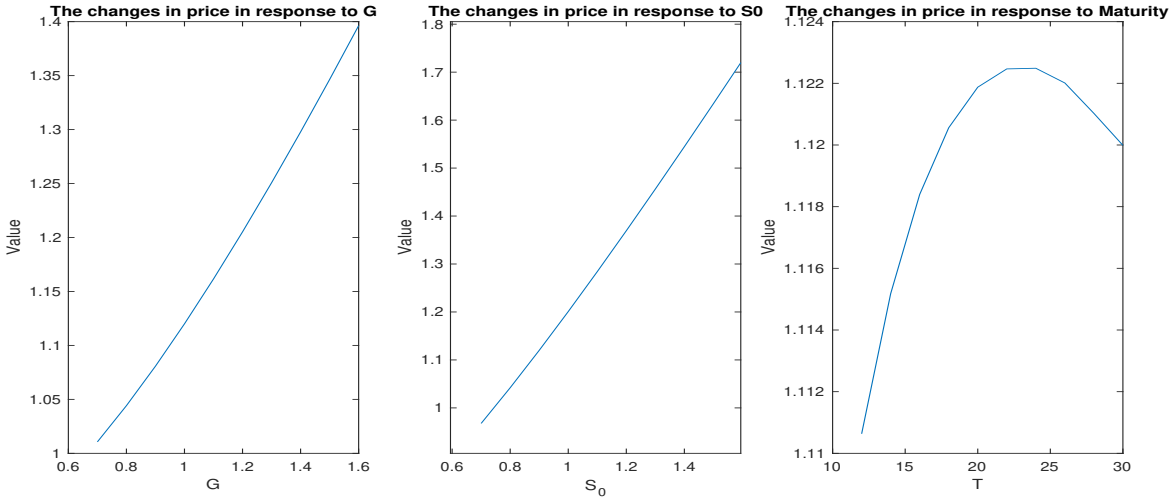

Figure 2: The sensitivity of VA prices with respect to G, S_0 and T. All other parameters are as presented in Table 1.

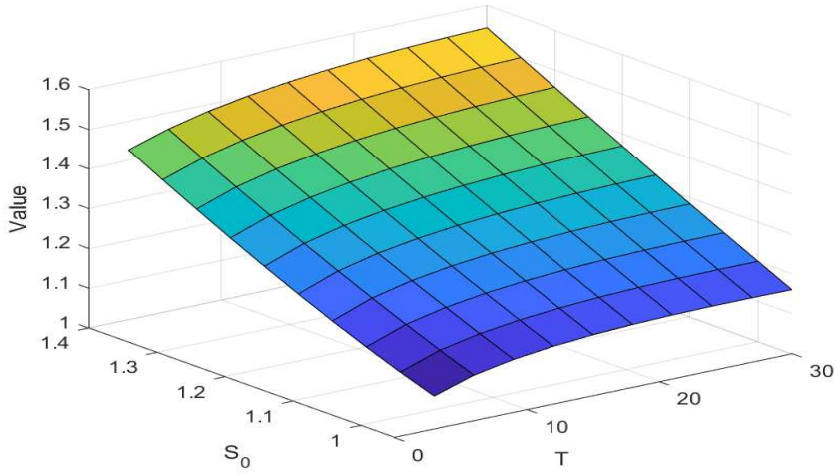

Figure 3: The sensitivity of VA prices with respect to S_0 and T. All other parameters are as presented in Table 1.

In Figure 4, we present the sensitivity of the VA prices with respect to G for varying maturities. From this figure, we note that deep in-the-money guarantees are more expensive relative to contracts with lower guarantees as the provider will have higher risk exposure. One key finding to note from all the subplots of Figure 4 is that for lower guarantees, longer maturity contracts are more expensive relative to shorter maturity contracts. However, as the guaranteed amount increases, we note a shift with shorter maturity contracts becoming more expensive relative to longer maturity contracts.

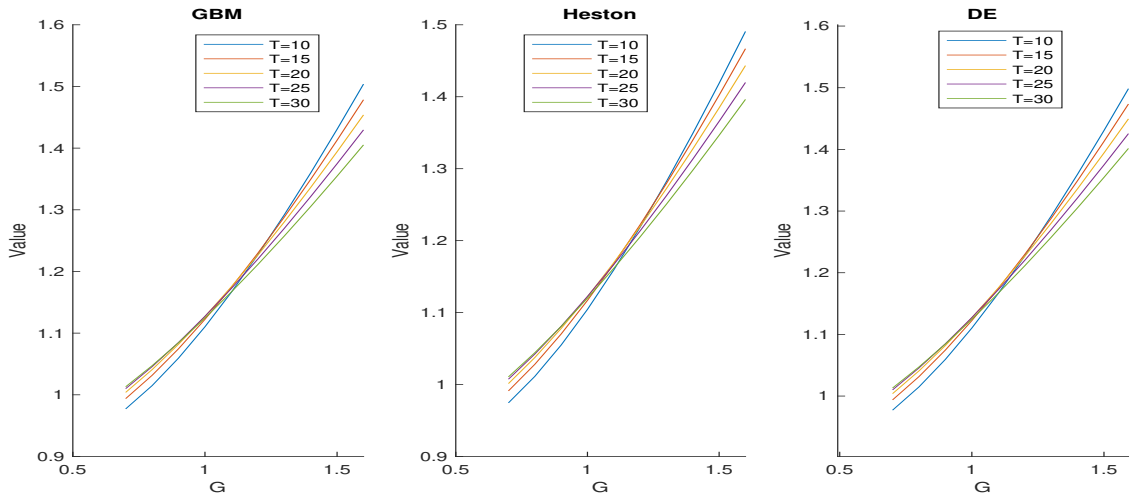

Figure 4: The sensitivity of VA prices with respect to G with different maturities and initial regimes. All other parameters are as presented in Table 1.

We now consider the effect of the transition intensities on the VA prices. In particular, we consider

$$A^* = \delta A,$$

where A is as defined in Equation (5.1). Figure 5 presents the values of the guarantee for varying intensity levels. As the intensity increases, the impact of the initial states diminishes. Under our parameter set-up, the prices produced by the GBM and the DE regimes are almost identical due to a relatively small Poisson intensity that we cannot differentiate as reflected on the left panel of Figure 5. Indeed, this finding is consistent with that in Figures 5-6 and 9-10 of Fan et al. (2015). On the right panel, we plot the difference in values where the underlying stock price dynamics start with the GBM and DE models, respectively, and it is evident from this plot that the differences are diminishing as the intensity grows. This is because with a larger intensity, different regimes are more likely to transition between each other, thereby less likely to stay the same. Then, the impact of the initial regimes on the VA prices will diminish.

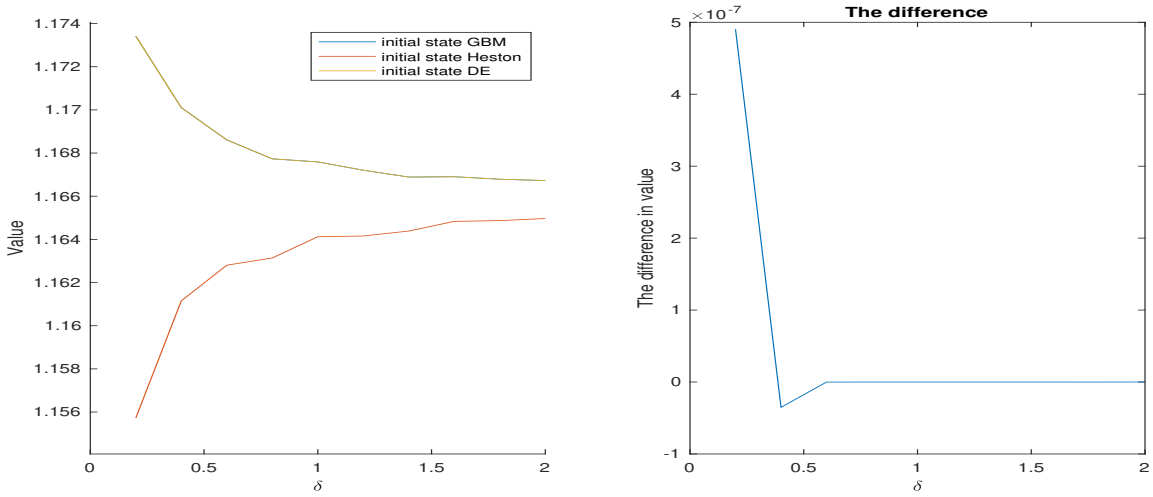

Figure 5: The sensitivity of VA prices with respect to intensity level. The price differences on the right panel are computed as the price of the GMB initial state minus the price of the DE initial state. All other parameters are as presented in Table 1.

5.2 Variable annuity embedded with ratchet geometric average GMMB

This subsection presents numerical illustrations for the VA contract embedded with a GMMB whose guarantee has ratchet features as presented in Subsection 4.2. To be more precise, we consider the payoff function

$$\vartheta(S_T, G_T) = \max\left\{\left(\prod_{m=0}^{T} S_m\right)^{\frac{1}{T+1}}, S_T\right\},$$

where the underlying fund dynamics are governed by a three-regime model. It is worth highlighting that the ratchet features are very distinct to the fixed and roll-up guarantees presented in Subsection 5.1 above. As such, for all numerical experiments that follow, we will assume that in each of the three states, the underlying fund evolves according to the Heston (1993) stochastic volatility process (refer to Example 2.2 for details about the three-regime Heston model). For illustrative purposes, we will consider a transition intensity matrix presented in Equation (5.1) and base parameters presented in Table 5.

Regime	1	2	3
	$r_1 = 0.01$	$r_2 = 0.02$	$r_3 = 0.03$
	$\theta_1 = 0.04$	$\theta_2 = 0.05$	$\theta_3 = 0.06$

Table 5: Parameter set for all numerical experiments performed in Subsection 5.2. Unless otherwise stated, we assume that the initial stock price/underlying fund value is $S_0 = 0.9$, the initial guarantee $G = 1$ and maturity $T = 15$. Across all three regimes, we assume the following parameters for the Heston (1993) stochastic volatility model: $V_0 = 0.04$, $\sigma_v = 0.05$, $\kappa = 10$, and $\rho = 0.5$.

Figure 6 presents the convergence analysis for the guarantee with ratchet features. We take the benchmark solution as that generated by the COS method computed with $N = 2^{11}$ grid points. From the left and right plots of Figure 6, we note a high convergence rate of the COS method with approximately 50 grid points and the linear relationship between $-\log(|\epsilon|)$ and $\log(N)$, which are consistent with the analysis and findings presented in Subsection 5.1.1.

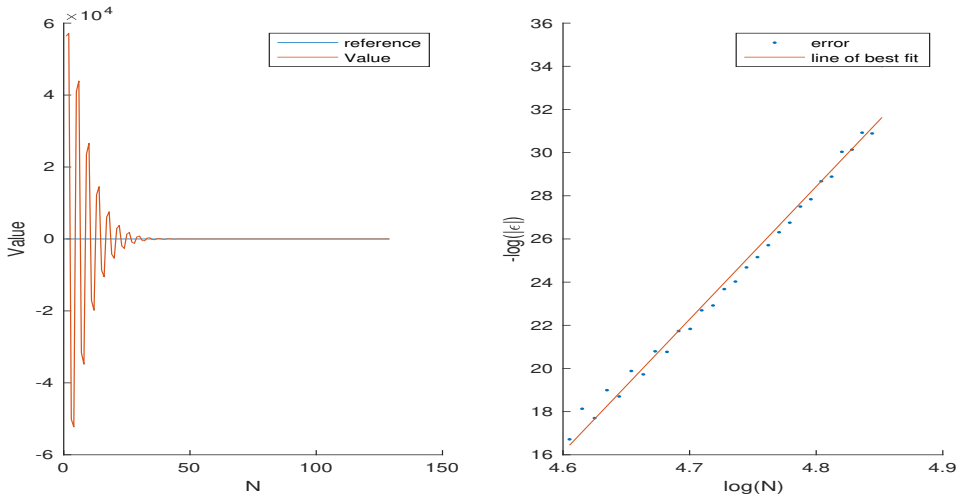

Figure 6: The convergence of the COS approach for GMMB with ratchet features. We consider the case with the geometric average floating strike guarantee presented in Subsection 4.2. The line of best fit is $-\log(|\epsilon|) = -266.92 + 61.633\log(N)$. The reference is taken from the value computed via the COS method using $N = 2^{11}$. All other parameters used for generating the plots are as presented in Table 5.

Having performed convergence tests, next, we assess the sensitivity of the variable annuity contract prices relative to changes in the underlying state variables. From the left plot of Figure 7, we note that the variable annuity contract price increases linearly with an increasing initial value of the fund. This is logical as there will be a higher probability of higher guarantees which are directly related to the fund value through the ratchet feature. From the middle plot of Figure 7, we note concave/hump-shaped sensitivity of the contract price with respect to the maturity of contract, which is again consistent with the fixed guarantee case in Subsection 5.1.1. The contract price is an increasing function of the initial instantaneous variance, V_0 as reflected on the right plot of Figure 7.

Shocking the intensity matrix has varying impact on the variable annuity contract prices as reflected in Figure 8. We note that the VA contract prices are divergent with different initial regimes when δ is relatively low. As the intensity increases, the differences are diminishing, which is consistent with the finding in Subsection 5.1. In the terminology of Fan et al. (2015), the blue line corresponds to a good initial state (regime), where the guarantee is relatively cheaper than those in the other two initial states. The optimism in the good state may mislead the VA provider to underestimate the likelihood of a transition from the current state to a bad one. Then such underestimation of the transition intensity would undervalue the VA contract. Therefore, the

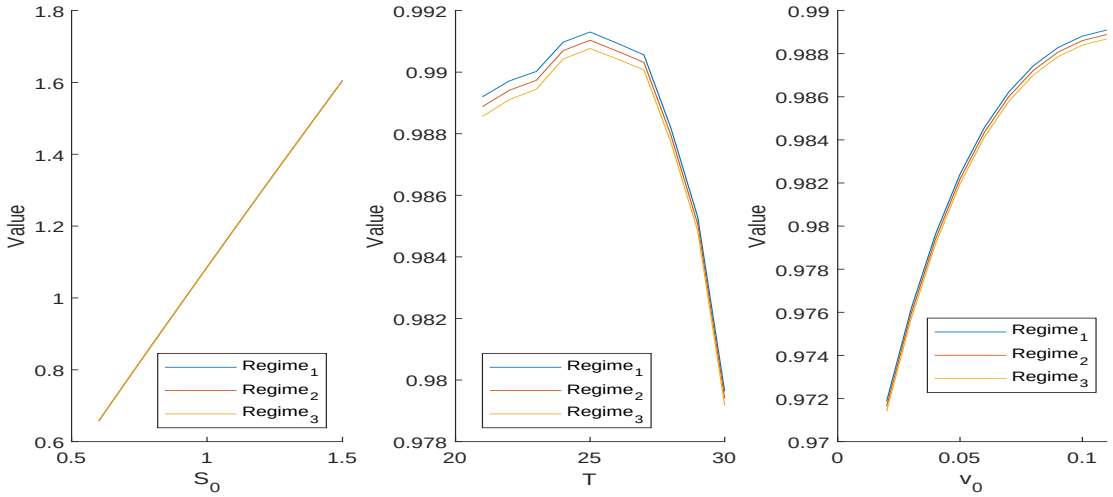

Figure 7: The sensitivity of the VA price with respect to S_0, T and V_0. All other parameters used for generating the plots are as presented in Table 5.

VA contract provider should be cautious about the outlook of market regimes.

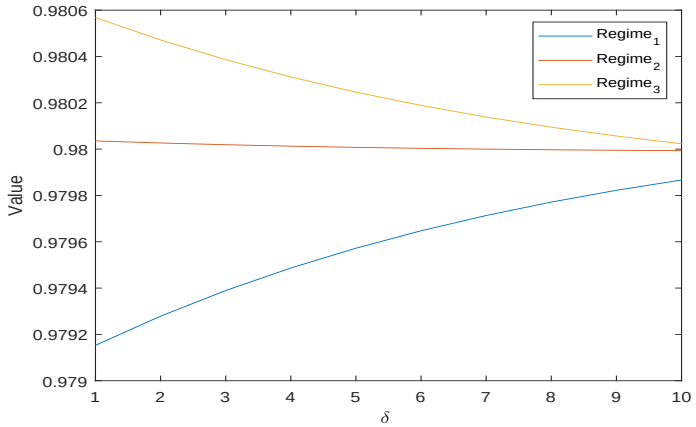

Figure 8: The sensitivity of the VA price with respect to intensity level. All other parameters used for generating the plots are as presented in Table 5.

We wrap up the analysis by providing a surface plot on how contract price reacts to changes in the initial variance and maturity in Figure 9 when all other parameters are as presented in Table 5 above. The trend is the same, that is, increasing V_0 implies increasing value. However, the effect of maturity is so strong that one cannot visually tell the trend in the other dimension. If one focuses at say, $T = 30$, the increasing trend in V_0 is evident.

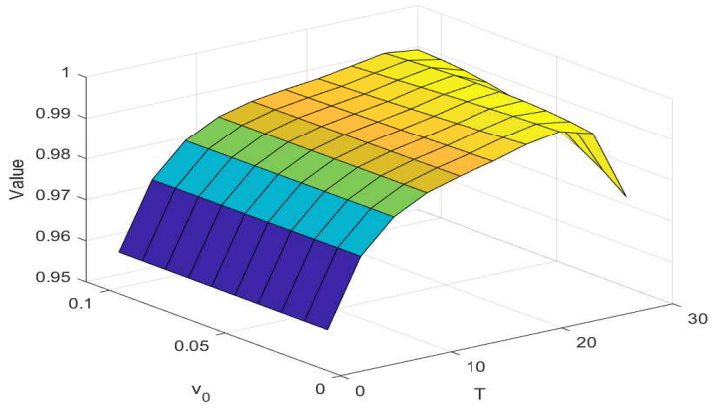

Figure 9: The sensitivity of the VA price with respect to V_0 and T. All other parameters used for generating the plots are as presented in Table 5.

6 Conclusion

This paper has considered the valuation of variable annuity contracts embedded with guaranteed minimum maturity benefit riders whose underlying fund evolves according to generalised regime-switching models. The environment in each regime is assumed to have distinct features, such as the underlying process driving the dynamics of the fund. We presented two illustrative examples whose regimes can be characterised by either the geometric Brownian motion process, double exponential process or Heston (1993) stochastic volatility process.

For the GMMB riders, we considered two distinct cases: a fixed guarantee that shares similar characteristics with roll-up guarantees and the second being a guarantee with ratchet features involving the geometric average of the historical fund value until maturity of the contract. Explicit valuation expressions for variable annuity contracts embedded with fixed and ratchet guarantees have been derived with the aid of the Fourier Cosine method, which is a proven versatile technique widely known for its computational efficiency in terms of speed and accuracy.

Efficiency tests for the valuation framework have been analysed relative to Monte Carlo simulation, and an algorithm for establishing the optimal number of grid points associated with the convergence of the COS method has been presented. Prior literature has mainly relied on ad hoc techniques when implementing the COS method.

Various sensitivity tests assessing how the variable annuity prices respond to changes in the key underlying variables such as contract maturity, guarantee level, transition intensity matrix, among others, have been presented, highlighting the impact of such changes.

References

J. Alonso-García, O. Wood, J. Ziveyi. Pricing and hedging guaranteed minimum withdrawal benefits under a general Lévy framework using the COS method. *Quantitative Finance*, 18(6):1049–1075, 2018.

J. Alonso-García, M. Sherris, S. Thirurajah, J. Ziveyi. Taxation and policyholder behavior: The case of guaranteed minimum accumulation benefits. Available at SSRN 3629101, 2020.

D. Bauer, A. Kling, J. Russ. A universal pricing framework for guaranteed minimum benefits in variable annuities. *ASTIN Bulletin*, 38(2):621–651, 2008.

T. Moenig, D. Bauer, D. Revisiting the risk-neutral approach to optimal policyholder behavior: A study of withdrawal guarantees in variable annuities. *Review of Finance*, 20(2):759–794, 2016.

L. Ballotta, E. Eberlein, T. Schmidt, R. Zeineddine. Variable annuities in a Lévy-based hybrid model with surrender risk. *Quantitative Finance*, 20(5):867–886, 2020.

F. Black, M. Scholes. The pricing of corporate liabilities *Journal of Political Economy*, 81:637–659, 1973.

C. Bernard, A. MacKay, M. Muehlbeyer. Optimal surrender policy for variable annuity guarantees. *Insurance: Mathematics and Economics*, 55:116–128, 2014.

D.S. Bernstein, W. So. Some explicit formulas for the matrix exponential. *IEEE Transactions on Automatic Control*, 38(8):1228-1232, 1993.

K.W. Chau, S.C.P. Yam, H. Yang. Fourier-cosine method for Gerber–Shiu functions. *Insurance: Mathematics and Economics*, 61:170–180, 2015.

M. Dai, Y.K. Kwok, J. Zong. Guaranteed minimum withdrawal benefit in variable annuities. *Mathematical Finance*, 18(4):595–611, 2008.

T.S. Dai, S.S. Yang, L.C. Liu. Pricing guaranteed minimum/lifetime withdrawal benefits with various provisions under investment, interest rate and mortality risks. *Insurance: Mathematics and Economics*, 64:364–379, 2015.

G. Deelstra, G. Rayée. Pricing variable annuity guarantees in a local volatility framework. *Insurance: Mathematics and Economics*, 53(3):650–663, 2013.

J. Da Fonseca, J. Ziveyi. Valuing variable annuity guarantees on multiple assets. *Scandinavian Actuarial Journal*, 2017(3):209–230, 2017.

R.J. Elliott, L. Aggoun, J.B. Moore. *Hidden Markov Models: Estimation and Control*. Springer, Berlin, Heidelberg, New York, 1994.

R.J. Elliott, L. Chan, T.K. Siu. Option pricing and Esscher transform under regime switching. *Annals of Finance*, 1:423–432, 2005.

R.J. Elliott, G. Lian. Pricing variance and volatility swaps in a stochastic volatility model with regime switching: Discrete observations case. *Quantitative Finance*, 13(5):687–698, 2013

K. Fan, Y. Shen, T.K. Siu, R. Wang. Pricing annuity guarantees under a double regime-switching model. *Insurance: Mathematics and Economics*, 62:62–78, 2015.

F. Fang, C.W. Oosterlee. A novel pricing method for European options based on Fourier-cosine series expansions. *SIAM Journal on Scientific Computing*, 31(2):826–848, 2008.

R. Feng, X. Jing. Analytical valuation and hedging of variable annuity guaranteed lifetime withdrawal benefits. *Insurance: Mathematics and Economics*, 72:36–48, 2017.

N. Gudkov, K. Ignatieva, J. Ziveyi. Pricing of guaranteed minimum withdrawal benefits in variable annuities under stochastic volatility, stochastic interest rates and stochastic mortality via the componentwise splitting method. *Quantitative Finance*, 19(3):501–518, 2019.

S.L. Heston. A closed-form solution for options with stochastic volatility with applications to bond and currency options. *The Review of Financial Studies*, 6(2):327–343, 2021.

K. Ignatieva, A. Song, J. Ziveyi. Pricing and hedging of guaranteed minimum benefits under regime-switching and stochastic mortality. *Insurance: Mathematics and Economics*, 70:286–300, 2016.

K. Ignatieva, A. Song, J. Ziveyi. Fourier space time-stepping algorithm for valuing guaranteed minimum withdrawal benefits in variable annuities under regime-switching and stochastic mortality. *ASTIN Bulletin*, 48(1):139–169, 2018.

B. Kang, J. Ziveyi. Optimal surrender of guaranteed minimum maturity benefits under stochastic volatility and interest rates. *Insurance: Mathematics and Economics*, 79:43–56, 2018.

A. Kélani, F. Quittard-Pinon. Pricing and hedging variable annuities in a Lévy market: A risk management perspective. *Journal of Risk and Insurance*, 84(1):209–238, 2017.

S.G. Kou, H. Wang. Option pricing under a double exponential jump diffusion model. *Management Science*, 50(9):1178–1192, 2004.

X. Li, Y. Shi, S.C.P. Yam, H. Yang. Fourier–cosine method for finite–time Gerber–Shiu functions. *SIAM Journal on Scientific Computing*, 43(3):B650–B677, 2021.

R. Lord, C. Kahl. Complex logarithms in Heston-like models. *Mathematical Finance*, 20(4)::671–694, 2010.

R. Mamon, H. Xiong, Y. Zhao. The valuation of a guaranteed minimum maturity benefit under a regime-switching framework. *North American Actuarial Journal*, 1-26, 2020.

M.A. Milevsky, T.S. Salisbury. Financial valuation of guaranteed minimum withdrawal benefits. *Insurance: Mathematics and Economics*, 38(1):21–38, 2006.

P.V. Shevchenko, X. Luo. Valuation of variable annuities with guaranteed minimum withdrawal benefit under stochastic interest rate. *Insurance: Mathematics and Economics*, 76:104–117, 2017.

Y. Shen, K. Fan, T.K. Siu. Option valuation under a double regime-switching model. *Journal of Futures Markets*, 34(5):451–478, 2014.

Y. Shen, M. Sherris, J. Ziveyi. Valuation of guaranteed minimum maturity benefits in variable annuities with surrender options. *Insurance: Mathematics and Economics*, 69:127–137, 2016.

G. Tour, N. Thakoor, A.Q.M. Khaliq, D.Y. Tangman. COS method for option pricing under a regime-switching model with time-changed Lévy processes. *Quantitative Finance*, 18(4):673–692, 2018.

C. Yuan, X. Mao. Convergence of the Euler-Maruyama method for stochastic differential equations with Markovian switching. *Mathematics and Computers in Simulation*, 64:223–235, 2004.

A Review of classical regime-switching model

In this Appendix, we review the CRS model, namely, the regime-switching jump-diffusion model. Suppose that the stock price follows:

$$\frac{dS_t}{S_{t-}} = r(\alpha_t)dt + \sigma(\alpha_t)dW_t + \int_{\mathbb{R}_0} \left[e^{\xi(y,\alpha_t)} - 1\right]\widetilde{N}(dt, dy, \alpha_t), \tag{A.1}$$

where $r(\alpha_t)$, $\sigma(\alpha_t)$, and $\xi(y, \alpha_t)$ are the risk-free interest rate, the volatility and the jump ratio of the stock at time t, and are modulated by the chain as follows:

$$\begin{aligned} r(\alpha_t) &:= \langle r, \alpha_t \rangle, \quad r := (r_1, r_2, \ldots, r_n)^\top, \\ \sigma(\alpha_t) &:= \langle \sigma, \alpha_t \rangle, \quad \sigma := (\sigma_1, \sigma_2, \ldots, \sigma_n)^\top, \\ \xi(y, \alpha_t) &:= \langle \xi(y), \alpha_t \rangle, \quad \xi(y) := (\xi_1(y), \xi_2(y), \ldots, \xi_n(y))^\top. \end{aligned}$$

where

$$r_j := r(e_j), \quad \sigma_j := \sigma(e_j), \quad \xi_j(y) := \xi(y, e_j).$$

By convention, we assume that $r_j > 0$, $\sigma_j > 0$ and $\xi_j(y) > -1$, for all $j = 1, 2, \ldots, n$.

Denote by the log-stock price as $X_t := \log(S_t)$. Applying Itô's formula, we obtain the dynamics of $\{X_t\}_{t\in[0,T]}$:

$$dX_t = \mu(\alpha_t)dt + \sigma(\alpha_t)dW_t + \int_{\mathbb{R}_0} \xi(y, \alpha_t)\widetilde{N}(dt, dy, \alpha_t), \tag{A.2}$$

where

$$\mu(\alpha_t) := r(\alpha_t) - \frac{1}{2}\sigma^2(\alpha_t) - \int_{\mathbb{R}_0} \left[e^{\xi(y,\alpha_t)} - 1 - \xi(y, \alpha_t)\right]\nu(dy, \alpha_t). \tag{A.3}$$

Denote by

$$dX_t^j = \mu_j dt + \sigma_j dW_t + \int_{\mathbb{R}_0} \xi_j(y)\widetilde{N}_j(dt, dy), \tag{A.4}$$

where

$$\widetilde{N}_j(dt,dy) := \widetilde{N}(dt,dy,e_j) = N(dt,dy) - \nu_j(dy)dt. \tag{A.5}$$

Obviously, the CRS model is a special case of the GRS model, since

$$X_t = x_0 + \int_0^t \mu(\alpha_s)ds + \sigma(\alpha_s)dW_s + \int_{\mathbb{R}_0} \xi(y,\alpha_s)\widetilde{N}(ds,dy,\alpha_s) = x_0 + \sum_{j=1}^n \int_0^t \langle \alpha_s, e_j\rangle \, dX_s^j. \tag{A.6}$$

It can be shown that the characteristic functions of X_T^j and X_T and the discounted characteristic function of X_T are given by

$$\Phi^j(u;t,x) := \mathbb{E}^Q\big[e^{iuX_T^j}|X_t^j = x\big] = \exp\big\{iux + g^j(u,t)\big\}, \tag{A.7}$$

$$\Phi_{X_T}(u;t,x) := \mathbb{E}^Q\big[e^{iuX_T}|X_t = x\big] = e^{iux}\left\langle \alpha_t, \exp\big\{[-\mathrm{diag}(G(u)) + A](T-t)\big\}1_n\right\rangle, \tag{A.8}$$

and

$$\widetilde{\Phi}_{X_T}(u;t,x) := \mathbb{E}^Q\big[e^{-\int_t^T r(\alpha_s)ds}e^{iuX_T}|X_t = x\big] = e^{iux}\left\langle \alpha_t, \exp\big\{[-\mathrm{diag}(G(u)+r) + A](T-t)\big\}1_n\right\rangle, \tag{A.9}$$

where

$$G(u) := \big(G_1(u), G_2(u), \ldots, G_n(u)\big)^\top,$$

with

$$G_j(u) := -\left\{iu\mu_j - \frac{1}{2}u^2\sigma_j^2 + \int_{\mathbb{R}_0}\big(e^{iu\xi_j(y)} - 1 - iu\xi_j(y)\big)\nu_j(dy)\right\} = g_t^j(u,t),$$

and

$$g^j(u,t) = \left\{iu\mu_j - \frac{1}{2}u^2\sigma_j^2 + \int_{\mathbb{R}_0}\big(e^{iu\xi_j(y)} - 1 - iu\xi_j(y)\big)\nu_j(dy)\right\}(T-t),$$

for $j = 1, 2, \ldots, n$.

The generalised characteristic function is given by

$$\widehat{\Phi}_{X_T}(\mathbf{u},\mathbf{B};t,x) := \mathbb{E}^Q\big[e^{-\int_t^T r(\alpha_s)ds + iu_TX_T}B_T|X_t = x\big] = \Big\langle \exp\{A(T-t)\}\alpha_t, \widehat{\mathbf{\Psi}}(t,x,\alpha_t)\Big\rangle, \tag{A.10}$$

where

$$\widehat{\mathbf{\Psi}}(t,x,\alpha_t) = \big(\widehat{\Psi}_1(t,x,\alpha_t), \widehat{\Psi}_2(t,x,\alpha_t), \ldots \widehat{\Psi}_n(t,x,\alpha_t)\big)^\top \tag{A.11}$$

with

$$\widehat{\Psi}_j(t,x,\alpha_t) = e^{iu_jx}\left\langle \alpha_t, \exp\big\{[-\mathrm{diag}(G(u_j)+r) + A](T-t)\big\}1_n\right\rangle B_j. \tag{A.12}$$

B Technical proofs

B.1 Proof of Proposition 2.1

Proof. By Itô's formula, we have

$$\begin{aligned} d\Phi^j(u;t,X_t^j,\zeta_t) &= d\exp\Big\{iuX_t^j + g^j(u,t) + D(u,t,\zeta_t)\Big\} \\ &= \Phi^j(u;t,X_t^j,\zeta_t)\Big\{iudX_t^j + \big[g_t^j + D_t\big]dt + D_\zeta d\zeta_t - \frac{u^2}{2}d\Big\langle (X_t^j)^c, (X_t^j)^c\Big\rangle \\ &\quad + \frac{1}{2}\big[D_{\zeta\zeta} + (D_\zeta)^2\big]d\left\langle (\zeta_t)^c, (\zeta_t)^c\right\rangle + iuD_\zeta d\Big\langle (X_t^j)^c, (\zeta_t)^c\Big\rangle \end{aligned}$$

$$+\left(e^{iu\Delta X_t^j+\Delta D(u,t,\zeta_t)}-1-iu\Delta X_t^j-D_\zeta\Delta\zeta_t\right)\Big\}.$$

Here g_t^j, D_t, D_ζ, $D_{\zeta\zeta}$ are abbreviations for (partial) derivatives of $g^j(u,t)$ and $D(u,t,\zeta)$ with respect to the corresponding variables t and ζ; $(\cdot)^c$ denotes the continuous component of a process; $\langle\cdot,\cdot\rangle$ denotes the quadratic covariation of two processes; ΔY_t denotes $\Delta Y_t := Y_t - Y_{t-}$, for any generic (càdlàg) process $\{Y_t\}_{t\in[0,T]}$.

Denote by

$$\begin{aligned}
d\mathcal{L}^D[(t,X_t^j,\zeta_t)](u) :=\ & iudX_t^j+\left[g_t^j+D_t\right]dt+D_\zeta d\zeta_t-\frac{u^2}{2}d\left\langle (X_t^j)^c,(X_t^j)^c\right\rangle\\
&+\frac{1}{2}\left[D_{\zeta\zeta}+(D_\zeta)^2\right]d\left\langle(\zeta_t)^c,(\zeta_t)^c\right\rangle+iuD_\zeta d\left\langle (X_t^j)^c,(\zeta_t)^c\right\rangle\\
&+\left(e^{iu\Delta X_t^j+\Delta D(u,t,\zeta_t)}-1-iu\Delta X_t^j-D_\zeta\Delta\zeta_t\right)\\
=\ &\left\{\mathcal{A}^D[(t,X_t^j,\zeta_t)](u)+g_t^j\right\}dt+d\mathcal{M}_t^j, \qquad \text{(B.1)}
\end{aligned}$$

where $\mathcal{A}^D[(t,X_t^j,\zeta_t)](u)$ denotes the drift generator (minus g_t^j), and $\mathcal{M}_t^j$ is the martingale component of $\mathcal{L}^D[(t,X_t^j,\zeta_t^j)](u)$. Note that $\mathcal{M}_t^j$ is independent of the chain.

It follows from the definition that $\Phi^j(u;t,X_t^j,\zeta_t)$ is a Q-martingale. Hence,

$$\mathcal{A}^D[(t,X_t^j,\zeta_t)](u)=-g_t^j(u,t). \qquad \text{(B.2)}$$

Again by Itô's formula, we have

$$\begin{aligned}
de^{iuX_\nu+D(u,\nu,\zeta_\nu)} =\ & e^{iuX_\nu+D(u,\nu,\zeta_\nu)}\Big\{iudX_\nu+D_\nu d\nu+D_\zeta d\zeta_\nu-\frac{u^2}{2}d\left\langle(X_\nu)^c,(X_\nu)^c\right\rangle\\
&+\frac{1}{2}\left[D_{\zeta\zeta}+(D_\zeta)^2\right]d\left\langle(\zeta_\nu)^c,(\zeta_\nu)^c\right\rangle+iuD_\zeta d\left\langle(X_\nu)^c,(\zeta_\nu)^c\right\rangle\\
&+\left(e^{iu\Delta X_\nu+\Delta D(u,t,\zeta_\nu)}-1-iu\Delta X_\nu-D_\zeta\Delta\zeta_\nu\right)\Big\}\\
=\ & e^{iuX_\nu+D(u,\nu,\zeta_\nu)}\sum_{j=1}^n\langle\alpha_\nu,e_j\rangle\Big\{iudX_\nu^j+D_\nu d\nu+D_\zeta d\zeta_\nu-\frac{u^2}{2}d\left\langle(X_\nu^j)^c,(X_\nu^j)^c\right\rangle\\
&+\frac{1}{2}\left[D_{\zeta\zeta}+(D_\zeta)^2\right]d\left\langle(\zeta_\nu)^c,(\zeta_\nu)^c\right\rangle+iuD_\zeta d\left\langle(X_\nu^j)^c,(\zeta_\nu)^c\right\rangle\\
&+\left(e^{iu\Delta X_\nu^j+\Delta D(u,t,\zeta_\nu)}-1-iu\Delta X_\nu^j-D_\zeta\Delta\zeta_\nu\right)\Big\}\\
=\ & e^{iuX_\nu+D(u,\nu,\zeta_\nu)}\sum_{j=1}^n\langle\alpha_\nu,e_j\rangle\left\{\mathcal{A}^D[(\nu,X_\nu^j,\zeta_\nu)](u)d\nu+d\mathcal{M}_\nu^j\right\}\\
=\ & e^{iuX_\nu+D(u,\nu,\zeta_\nu)}\sum_{j=1}^n\langle\alpha_\nu,e_j\rangle\left\{-g_\nu^j(u,\nu)d\nu+d\mathcal{M}_\nu^j\right\}.
\end{aligned}$$

By the stochastic product rule, we obtain

$$\begin{aligned}
d\left\{\alpha_\nu e^{-\int_0^\nu r_sds+iuX_\nu+D(u,\nu,\zeta_\nu)}\right\} =\ & \left\{-\mathrm{Diag}[G(u,t)+r]+A\right\}\alpha_\nu e^{-\int_0^\nu r_sds+iuX_\nu+D(u,\nu,\zeta_\nu)}d\nu\\
&+\alpha_\nu e^{-\int_0^\nu r_sds+iuX_\nu+D(u,\nu,\zeta_\nu)}\sum_{j=1}^n\langle\alpha_\nu,e_j\rangle\,d\mathcal{M}_\nu^j+e^{-\int_0^\nu r_sds+iuX_\nu+D(u,\nu,\zeta_\nu)}dm_\nu.
\end{aligned}$$

For $\nu\geq t$, conditioning on $\mathcal{F}_t$ gives

$$d\mathbb{E}^Q\left[\alpha_\nu e^{-\int_0^\nu r_sds+iuX_\nu+D(u,\nu,\zeta_\nu)}\Big|\mathcal{F}_t\right]=\left\{-\mathrm{Diag}[G(u,t)+r]+A\right\}\mathbb{E}^Q\left[\alpha_\nu e^{-\int_0^\nu r_sds+iuX_\nu+D(u,\nu,\zeta_\nu)}\Big|\mathcal{F}_t\right]d\nu.$$

Thus,

$$\mathbb{E}^Q\left[\alpha_T e^{-\int_0^T r_sds+iuX_T+D(u,T,\zeta_T)}\Big|\mathcal{F}_t\right]=\alpha_t e^{-\int_0^t r_sds+iuX_t+D(u,t,\zeta_t)}\Psi(u,t) \qquad \text{(B.3)}$$

and

$$\begin{aligned}\widetilde{\Phi}_{X_T}(u;t,x,\zeta) &= \mathbb{E}^Q\left[e^{-\int_t^T r_s ds + iuX_T} | X_t = x, \zeta_t = \zeta\right] \\ &= \mathbb{E}^Q\left[e^{-\int_t^T r_s ds + iuX_T} \langle \alpha_T, 1_n\rangle | X_t = x, \zeta_t = \zeta\right] \\ &= e^{iux + D(u,t,\zeta)} \langle \alpha_t, \Psi(u,t) 1_n\rangle, \end{aligned} \tag{B.4}$$

where $\Psi(u,t)$ is the fundamental solution to the matrix-valued ordinary differential equation (ODE) (2.11).

If $g_t^j(u,t)$ are all t-independent, for $j = 1, 2, \ldots, n$, then the fundamental solution can be expressed by exponential matrix as follows

$$\Psi(u,t) = \exp\left\{\left[-\mathrm{Diag}(G(u) + r) + A\right](T-t)\right\}. \tag{B.5}$$

Substituting (B.5) into (2.10) gives (2.13). □

B.2 Proof of Corollary 2.1

Proof. In this proof, let $\mathbb{E}^Q_{t,x,\zeta}[\cdot]$ and $\mathbb{E}^Q_{t,x,\zeta,\alpha_T}[\cdot]$ denote the conditional expectations $\mathbb{E}^Q\left[\,\cdot\,|X_t = x, \zeta_t = \zeta\right]$ and $\mathbb{E}^Q\left[\,\cdot\,|X_t = x, \zeta_t = \zeta, \alpha_T\right]$, respectively. Applying the tower property to the generalised characteristic function gives

$$\begin{aligned}\widehat{\Phi}_{X_T}(\mathbf{u}, \mathbf{B}; t, x, \zeta) &= \mathbb{E}^Q_{t,x,\zeta}\left[\mathbb{E}^Q_{t,x,\zeta,\alpha_T}\left[e^{-\int_t^T r_s ds + iu_T X_T} B_T\right]\right] \\ &= \mathbb{E}^Q_{t,x,\zeta}\left[\widetilde{\Phi}(u_T; t, x, \zeta) B_T\right] \\ &= \mathbb{E}^Q_{t,x,\zeta}\left[e^{iu_T x + D(u_T,t,\zeta)} \langle \alpha_t, \Psi(u_T, t) 1_n\rangle B_T\right] \\ &= \mathbb{E}^Q_{t,x,\zeta}\left[\left\langle \alpha_T, \widehat{\mathbf{\Psi}}(t,x,\zeta,\alpha_t)\right\rangle\right] \\ &= \left\langle \exp\{A(T-t)\}\alpha_t, \widehat{\mathbf{\Psi}}(t,x,\zeta,\alpha_t)\right\rangle. \end{aligned} \tag{B.6}$$

This completes the proof. □

B.3 Characteristic function for the ratchet option under CRS model

Recalling for both the CRS and GRS models, we have that for any integer m

$$X_m = X_0 + \sum_{i=1}^m x_i, \tag{B.7}$$

where

$$x_i := \sum_{j=1}^n \int_{i-1}^i \langle \alpha_s, e_j\rangle \, dX_s^j, \tag{B.8}$$

Define

$$x_i^j := \int_{i-1}^i dX_s^j = X_i^j - X_{i-1}^j. \tag{B.9}$$

By some algebraic manipulation, we proceed as follows:

$$\begin{aligned} Z_T = \log(G_T/S_T) = \log G_T - \log S_T &= \frac{1}{T+1}\sum_{m=0}^T \log S_m - \log S_T \\ = \frac{1}{T+1}\left(X_0 + \sum_{m=1}^T \left\{X_0 + \sum_{i=1}^m x_i\right\}\right) &- \left(X_0 + \sum_{m=1}^T x_m\right) \end{aligned}$$

$$
\begin{aligned}
&= \frac{1}{T+1}\sum_{m=1}^{T}\sum_{i=1}^{m} x_i - \sum_{m=1}^{T} x_m \\
&= \frac{1}{T+1}\sum_{m=1}^{T} x_m \sum_{i=m}^{T} 1 - \sum_{m=1}^{T} x_m \\
&= -\frac{1}{T+1}\sum_{m=1}^{T} m x_m, \qquad \text{(B.10)}
\end{aligned}
$$

where x_m for $m = 1, \cdots, T$ are the independent increments defined by (B.8).

Thus, the characteristic function of Z_T is

$$
\begin{aligned}
\Phi_{Z_T}(u) &:= \mathbb{E}^{\tilde{Q}}[e^{iuZ_T}] \\
&= \prod_{m=1}^{T} \mathbb{E}^{\tilde{Q}}\left[e^{-iu\frac{m}{T+1}x_m}\right] \\
&= \prod_{m=1}^{T} \Phi_{x_m}^{\tilde{Q}}\left(-u\frac{m}{T+1}\right), \qquad \text{(B.11)}
\end{aligned}
$$

where $\Phi_{x_m}^{\tilde{Q}}(u)$ is the characteristic function of x_m under $\tilde{Q}$.

To derive $\Phi_{x_m}^{\tilde{Q}}(u)$, we need to know the $\tilde{Q}$-dynamics of x_m and we have to derive these dynamics case by case. Subsequently, we consider the case given by the CRS model in this subsection and that by Example 2.2 in Subsection B.4.

Let us construct the $\tilde{Q}$ measure for the CRS model:

$$
\begin{aligned}
\left.\frac{d\tilde{Q}}{dQ}\right|_{\mathcal{F}_T} &= \eta_T = e^{-\int_0^T r_t dt}\frac{S_T}{S_0} \\
&= \exp\Big\{ -\frac{1}{2}\int_0^T \sigma^2(\alpha_t)dt - \int_0^T\int_{\mathbb{R}_0}\left[e^{\xi(y,\alpha_t)} - 1 - \xi(y,\alpha_t)\right]\nu(dy,\alpha_t)dt \\
&\quad + \int_0^T \sigma(\alpha_t)dW_t + \int_0^T\int_{\mathbb{R}_0}\xi(y,\alpha_t)\widetilde{N}(dt,dy,\alpha_t)\Big\}. \qquad \text{(B.12)}
\end{aligned}
$$

Hence, under $\tilde{Q}$,

$$
W_t^{\tilde{Q}} := W_t - \int_0^t \sigma(\alpha_s)ds \qquad \text{(B.13)}
$$

is a standard Brownian motion, the compensator of $N(dt,dy)$ becomes $e^{\xi(y,\alpha_t)}\nu(dy,\alpha_t)dt$, that is

$$
\widetilde{N}_j^{\tilde{Q}}(dt,dy) := \widetilde{N}^{\tilde{Q}}(dt,dy,e_j) = N(dt,dy) - e^{\xi_j(y)}\nu_j(dy)dt \qquad \text{(B.14)}
$$

are martingales, for $j = 1, 2, \ldots, n$, and the probability law of the chain α_t remains the same as that under Q.

Then, the $\tilde{Q}$-dynamics of the log-stock price process $\{X_t\}_{t\in[0,T]}$ is given by

$$
dX_t = b(\alpha_t)dt + \sigma(\alpha_t)dW_t^{\tilde{Q}} + \int_{\mathbb{R}_0}\xi(y,\alpha_t)\widetilde{N}^{\tilde{Q}}(dt,dy,\alpha_t), \qquad \text{(B.15)}
$$

where

$$
b(\alpha_t) := r(\alpha_t) + \frac{1}{2}\sigma^2(\alpha_t) + \nu(\mathbb{R}_0,\alpha_t). \qquad \text{(B.16)}
$$

For any integer m, we have the decomposition

$$
\log(S_m) = X_m = X_0 + \sum_{i=1}^{m} x_i, \qquad \text{(B.17)}
$$

where

$$x_i := \int_{i-1}^{i} b(\alpha_t)dt + \int_{i-1}^{i} \sigma(\alpha_t)dW_t^{\tilde{Q}} + \int_{i-1}^{i}\int_{\mathbb{R}_0} \xi(y,\alpha_t)\widetilde{N}^{\tilde{Q}}(dt,dy,\alpha_t). \tag{B.18}$$

By the tower property, we have

$$\Phi_{x_m}^{\tilde{Q}}(u) = \mathbb{E}^{\tilde{Q}}\left[e^{iux_m}\right] = \mathbb{E}^{\tilde{Q}}\left[\mathbb{E}^{\tilde{Q}}\left[e^{iux_m}|\mathcal{F}_m^{\alpha}\right]\right]. \tag{B.19}$$

Consider the inner conditional expectation first. It follows from the independence of the Brownian motion, the random measure and the chain that

$$\begin{aligned}\mathbb{E}^{\tilde{Q}}\left[e^{iux_m}|\mathcal{F}_m^{\alpha}\right] &= e^{\int_{m-1}^{m} iub(\alpha_t)dt}\cdot\mathbb{E}^{\tilde{Q}}\left[e^{\int_{m-1}^{m} iu\sigma(\alpha_t)dW_t^{\tilde{Q}}}|\mathcal{F}_m^{\alpha}\right]\cdot\mathbb{E}^{\tilde{Q}}\left[e^{\int_{m-1}^{m}\int_{\mathbb{R}_0} iu\xi(y,\alpha_t)\widetilde{N}^{\tilde{Q}}(dt,dy,\alpha_t)}|\mathcal{F}_m^{\alpha}\right]\\ &= \exp\left\{\int_{m-1}^{m}\left[iub(\alpha_t) - \frac{1}{2}u^2\sigma^2(\alpha_t) + \int_{\mathbb{R}_0}\left(e^{iu\xi(y,\alpha_t)} - 1 - iu\xi(y,\alpha_t)\right)e^{\xi(y,\alpha_t)}\nu(dy,\alpha_t)\right]dt\right\}.\end{aligned} \tag{B.20}$$

Denote by

$$\psi^j(u) := iub_j - \frac{1}{2}u^2\sigma_j^2 + \int_{\mathbb{R}_0}\left(e^{iu\xi_j(y)} - 1 - iu\xi_j(y)\right)e^{\xi_j(y)}\nu_j(dy) \tag{B.21}$$

and

$$\psi(u) := \left(\psi^1(u), \psi^2(u), \ldots, \psi^n(u)\right)^{\top}. \tag{B.22}$$

Substituting (B.21) into (B.19) and using the tower property again yields

$$\begin{aligned}\Phi_{x_m}^{\tilde{Q}}(u) &= \mathbb{E}^{\tilde{Q}}\left[\mathbb{E}^{\tilde{Q}}\left[\mathbb{E}^{\tilde{Q}}\left[e^{iux_m}|\mathcal{F}_m^{\alpha}\right]\langle\alpha_m, 1_n\rangle\,\middle|\mathcal{F}_{m-1}^{\alpha}\right]\right]\\ &= \mathbb{E}^{\tilde{Q}}\left[\left\langle\alpha_{m-1}, \exp\left\{\left[\mathrm{diag}(\psi(u)) + A\right]\right\}1_n\right\rangle\right]\\ &= \left\langle\exp\{A(m-1)\}\alpha_0, \exp\left\{\left[\mathrm{diag}(\psi(u)) + A\right]\right\}1_n\right\rangle.\end{aligned} \tag{B.23}$$

Therefore,

$$\Phi_{Z_T}(u) = \prod_{m=1}^{T}\left\langle\exp\{A(m-1)\}\alpha_0, \exp\left\{\left[\mathrm{diag}\left(\psi\left(-u\frac{m}{T+1}\right)\right) + A\right]\right\}1_n\right\rangle, \tag{B.24}$$

and the generalised characteristic function of Z_T is given by

$$\widehat{\Phi}_{Z_T}(\mathbf{c}(k), \mathbf{H}(k)) = \left\langle\exp\{A\cdot T\}\alpha_0, \widehat{\mathbf{\Psi}}\right\rangle, \tag{B.25}$$

where $\widehat{\mathbf{\Psi}} = (\widehat{\Psi}_1, \widehat{\Psi}_2, \ldots, \widehat{\Psi}_n)^{\top}$ with

$$\widehat{\Psi}_j = \prod_{m=1}^{T}\left\langle\exp\{A(m-1)\}\alpha_0, \exp\left\{\left[\mathrm{diag}\left(\psi\left(-c_j(k)\frac{m}{T+1}\right)\right) + A\right]\right\}1_n\right\rangle H_j(k). \tag{B.26}$$

B.4 Characteristic function for the ratchet option under Example 2.2

Under Example 2.2, the $\tilde{Q}$ measure is equivalent to Q as follows:

$$\begin{aligned}\left.\frac{d\tilde{Q}}{dQ}\right|_{\mathcal{F}_T} &= \eta_T = e^{-\int_0^T r_t dt}\frac{S_T}{S_0}\\ &= \exp\left\{-\sum_{j=1}^{n}\int_0^T \frac{1}{2}\langle\alpha_t, e_j\rangle V_t^j dt + \sum_{j=1}^{n}\int_0^T \langle\alpha_t, e_j\rangle\sqrt{V_t^j}dW_t\right\}.\end{aligned} \tag{B.27}$$

Hence, under $\tilde{Q}$,

$$W_t^{\tilde{Q}} := W_t - \sum_{j=1}^{n} \int_0^t \langle \alpha_s, e_j \rangle \sqrt{V_s^j}\, ds \tag{B.28}$$

is a standard Brownian motion, and the probability laws of the Brownian motion $\bar{W}_t = \bar{W}_t^{\tilde{Q}}$ and the Markov chain α_t remain unchanged.

Under the $\tilde{Q}$ measure, the log-stock price process and the variance process follow

$$dX_t^j = \left(r_j + \frac{1}{2}V_t^j\right)dt + \sqrt{V_t^j}\, dW_t^{\tilde{Q}} \tag{B.29}$$

and

$$dV_t^j = \left[\kappa\theta_j + (\rho\sigma_v - \kappa)V_t^j\right] + \sqrt{V_t^j}\sigma_v\left[\rho dW_t^{\tilde{Q}} + \sqrt{1-\rho^2}\, d\bar{W}_t^{\tilde{Q}}\right]. \tag{B.30}$$

The characteristic function of X_t^j is given by

$$\Phi^j(u;t,T,x,\zeta) = \mathbb{E}^{\tilde{Q}}[e^{iuX_T^j} | X_t^j = x, V_t^j = \zeta] = \exp\left\{iux + \tilde{g}^j(u;t,T) + \tilde{D}(u,t,T)\zeta\right\}, \tag{B.31}$$

where

$$\tilde{g}^j(u;t,T) = iur_j\tau + \tilde{C}^j(u,t,T), \tag{B.32}$$

and $\tilde{C}^j(u,t,T)$ and $\tilde{D}(u,t,T)$ are to be determined below.

Applying Itô's formula yields

$$\begin{aligned}
&d\Phi^j(u;t,T,X_t^j,V_t^j)\\
&= d\exp\left\{iuX_t^j + \tilde{g}^j(u;t,T) + \tilde{D}(u,t,T)V_t^j\right\}\\
&= \Phi^j(u;t,T,X_t^j,V_t^j)\Big\{iudX_t^j - \frac{1}{2}u^2V_t^j dt + \left[-iur_2 + \tilde{C}_t^j(u,t,T) + \tilde{D}_t(u,t,T)V_t^j\right]dt + \tilde{D}(u,t,T)dV_t^j\\
&\qquad\qquad + \frac{1}{2}\tilde{D}^2(u,t,T)V_t^j\sigma_v^2 dt + \tilde{D}(u,t,T)V_t^j iu\sigma_v\rho dt\Big\}\\
&= \Phi^j(u;t,T,X_t^j,V_t^j)\Big\{\left[\frac{1}{2}\left(iu - u^2\right) + \tilde{D}_t(u,t,T) + (\rho\sigma_v - \kappa + iu\sigma_v\rho)\tilde{D}(u,t,T) + \frac{1}{2}\sigma_v^2\tilde{D}^2(u,t,T)\right]V_t^j dt\\
&\quad + \left[\tilde{C}_t^j(u,t,T) + \kappa\theta_j\tilde{D}(u,t,T)\right]dt + \left[iu\sqrt{V_t^j} + \tilde{D}(u,t,T)V_t^j\sigma_v\rho\right]dW_t^{\tilde{Q}} + \tilde{D}(u,t,T)V_t^j\sigma_v\sqrt{1-\rho^2}\, d\bar{W}_t^{\tilde{Q}}\Big\}.
\end{aligned}$$

Since $\Phi^j(u;t,T,X_t^j,V_t^j)$ is a $\tilde{Q}$-martingale, setting the drift to be zero gives that $\tilde{C}^j(u,t,T)$ and $\tilde{D}(u,t,T)$ satisfy the following ODEs:

$$\tilde{C}_t^j(u,t,T) + \kappa\theta_j\tilde{D}(u,t,T) = 0, \quad \tilde{C}(u,T,T) = 0, \tag{B.33}$$

and

$$\tilde{D}_t(u,t,T) - \left(\kappa - (1+iu)\rho\sigma_v\right)\tilde{D}(u,t,T) + \frac{1}{2}\sigma_v^2\tilde{D}^2(u,t,T) - \frac{1}{2}(-iu + u^2) = 0, \quad \tilde{D}(u,T,T) = 0. \tag{B.34}$$

Let us first consider (B.34), which is a Riccati equation with complex-valued coefficients. To that end, we try the following *ansatz*

$$\tilde{D}(u,t,T) = \frac{R_2(\tau)}{R_1(\tau)}, \quad \tau := T - t, \tag{B.35}$$

with initial conditions $R_1(0) = 1$ and $R_2(0) = 0$.

Using the product rule to $R_2(\tau) = \tilde{D}(u,t,T)R_1(\tau)$, together with (B.34), we obtain

$$\frac{dR_2(\tau)}{d\tau} = R_1(\tau)\frac{d\tilde{D}(u,t,T)}{d\tau} + \tilde{D}(u,t,T)\frac{dR_1(\tau)}{d\tau}$$

$$= R_1(\tau)\Big[-\big(\kappa - (1+iu)\rho\sigma_v\big)\tilde{D}(u,t,T) + \frac{1}{2}\sigma_v^2\tilde{D}^2(u,t,T) - \frac{1}{2}(-iu+u^2)\Big] + \tilde{D}(u,t,T)\frac{dR_1(\tau)}{d\tau}$$
$$= -\big(\kappa - (1+iu)\rho\sigma_v\big)R_2(\tau) + \frac{1}{2}\sigma_v^2\tilde{D}(u,t,T)R_2(\tau) - \frac{1}{2}(-iu+u^2)R_1(\tau) + \tilde{D}(u,t,T)\frac{dR_1(\tau)}{d\tau}. \quad \text{(B.36)}$$

Then matching the coefficients of $\tilde{D}(u,t,T)$ yields

$$\frac{dR_1(\tau)}{d\tau} = -\frac{1}{2}\sigma_v^2 R_2(\tau), \quad R_1(0) = 1, \quad \text{(B.37)}$$
$$\frac{dR_1(\tau)}{d\tau} = -\frac{1}{2}(-iu+u^2)R_1(\tau) - \big(\kappa - (1+iu)\rho\sigma_v\big)R_2(\tau), \quad R_2(0) = 0. \quad \text{(B.38)}$$

Let us rewrite the above system of ODEs in the vector-matrix form

$$d\begin{pmatrix} R_1(\tau) \\ R_2(\tau) \end{pmatrix} = \begin{pmatrix} 0 & -\frac{1}{2}\sigma_v^2 \\ -\frac{1}{2}(-iu+u^2) & -\big(\kappa - (1+iu)\rho\sigma_v\big) \end{pmatrix}\begin{pmatrix} R_1(\tau) \\ R_2(\tau) \end{pmatrix} d\tau. \quad \text{(B.39)}$$

The solution of (B.39) is given by

$$\begin{pmatrix} R_1(\tau) \\ R_2(\tau) \end{pmatrix} = \exp\left\{\begin{bmatrix} 0 & -\frac{1}{2}\sigma_v^2 \\ -\frac{1}{2}(-iu+u^2) & -\big(\kappa - (1+iu)\rho\sigma_v\big) \end{bmatrix}\tau\right\}\begin{pmatrix} 1 \\ 0 \end{pmatrix}. \quad \text{(B.40)}$$

Hence, using the results in Bernstein and So (1993) and some simple algebra, we have

$$R_1(\tau) = e^{-\frac{1}{2}(\kappa-(1+iu)\rho\sigma_v)\tau}\cdot\left(\cosh(\delta\tau) + \frac{\kappa-(1+iu)\rho\sigma_v}{2\delta}\sinh(\delta\tau)\right) \quad \text{(B.41)}$$

and

$$R_2(\tau) = e^{-\frac{1}{2}(\kappa-(1+iu)\rho\sigma_v)\tau}\cdot\left(-\frac{-iu+u^2}{2\delta}\sinh(\delta\tau)\right), \quad \text{(B.42)}$$

where

$$\delta = \frac{1}{2}\sqrt{\big(\kappa-(1+iu)\rho\sigma_v\big)^2 + \sigma_v^2(-iu+u^2)}. \quad \text{(B.43)}$$

Therefore, plugging the above two expressions into (B.35) and rearranging to get the formulation as in Lord and Kahl (2010), we derive

$$\begin{aligned}
\tilde{D}(u;t,T) &= \frac{-\frac{-iu+u^2}{2\delta}\sinh(\delta\tau)}{\cosh(\delta\tau) + \frac{\kappa-(1+iu)\rho\sigma_v}{2\delta}\sinh(\delta\tau)} \\
&= \frac{-(-iu+u^2)}{2\delta\frac{\cosh(\delta\tau)}{\sinh(\delta\tau)} + (\kappa-(1+iu)\rho\sigma_v)} \\
&= \frac{-(-iu+u^2)(1-e^{-2\delta\tau})}{2\delta(1+e^{-2\delta\tau}) + (\kappa-(1+iu)\rho\sigma_v)(1-e^{-2\delta\tau})} \\
&= \frac{\frac{1}{\sigma_v^2}[(\kappa-(1+iu)\rho\sigma_v)^2 - \tilde{d}^2(u)](1-e^{-\tilde{d}(u)\tau})}{(\kappa-(1+iu)\rho\sigma_v+\tilde{d}(u)) - (\kappa-(1+iu)\rho\sigma_v-\tilde{d}(u))e^{-\tilde{d}(u)\tau}} \\
&= \frac{(\kappa-(1+iu)\rho\sigma_v+\tilde{d}(u))(1-e^{-\tilde{d}(u)\tau})}{\sigma_v^2[\tilde{c}(u)-e^{-\tilde{d}(u)\tau}]} \\
&= \frac{\kappa-(1+iu)\rho\sigma_v+\tilde{d}(u)}{\sigma_v^2\tilde{c}(u)}\frac{1-e^{-\tilde{d}(u)\tau}}{1-e^{-\tilde{d}(u)\tau}/\tilde{c}(u)} \\
&= \frac{\kappa-(1+iu)\rho\sigma_v-\tilde{d}(u)}{\sigma_v^2}\frac{1-e^{-\tilde{d}(u)\tau}}{1-e^{-\tilde{d}(u)\tau}/\tilde{c}(u)}
\end{aligned}$$

$$= \frac{\kappa - (1+iu)\rho\sigma_v - \tilde{d}(u)}{\sigma_v^2} \frac{1 - e^{-\tilde{d}(u)\tau}}{1 - \hat{c}(u)e^{-\tilde{d}(u)\tau}},$$

where

$$\tilde{c}(u) = \frac{\kappa - (1+iu)\rho\sigma_v + \tilde{d}(u)}{\kappa - (1+iu)\rho\sigma_v - \tilde{d}(u)}, \quad \hat{c}(u) = \frac{1}{\tilde{c}(u)},$$
$$\tilde{d}(u) = 2\delta = \sqrt{\big(\kappa - (1+iu)\rho\sigma_v\big)^2 + \sigma_v^2(-iu + u^2)}.$$

On the other hand, we have

$$\begin{aligned}
\tilde{C}^j(u,t,T) &= \kappa\theta_j \int_t^T \tilde{D}(u,s,T)ds \\
&= \kappa\theta_j \int_t^T \frac{R_2(T-s)}{R_1(T-s)}ds = \frac{2\kappa\theta_j}{\sigma_v^2}\int_t^T \frac{dR_1(T-s)}{R_1(T-s)} = -\frac{2\kappa\theta_j}{\sigma_v^2}\log R_2(\tau) \\
&= -\frac{2\kappa\theta_j}{\sigma_v^2}\bigg[-\frac{1}{2}\big(\kappa - (1+iu)\rho\sigma_v\big)\tau + \log\bigg(\cosh(\delta\tau) + \frac{\kappa - (1+iu)\rho\sigma_v}{2\delta}\sinh(\delta\tau)\bigg)\bigg] \\
&= \frac{\kappa\theta_j}{\sigma_v^2}\bigg[\big(\kappa - (1+iu)\rho\sigma_v\big)\tau - 2\log\bigg(\frac{2\delta(e^{\delta\tau} + e^{-\delta\tau}) + \big(\kappa - (1+iu)\rho\sigma_v\big)(e^{\delta\tau} - e^{-\delta\tau})}{4\delta}\bigg)\bigg] \\
&= \frac{\kappa\theta_j}{\sigma_v^2}\bigg[\big(\kappa - (1+iu)\rho\sigma_v\big)\tau - 2\log\bigg(e^{-\delta\tau}\frac{e^{2\delta\tau}\tilde{c}(u) - 1}{\tilde{c}(u) - 1}\bigg)\bigg] \\
&= \frac{\kappa\theta_j}{\sigma_v^2}\bigg[\big(\kappa - (1+iu)\rho\sigma_v + \tilde{d}(u)\big)\tau - 2\log\bigg(\frac{1 - e^{\tilde{d}(u)\tau}\tilde{c}(u)}{1 - \tilde{c}(u)}\bigg)\bigg] \\
&= \frac{\kappa\theta_j}{\sigma_v^2}\bigg[\big(\kappa - (1+iu)\rho\sigma_v + \tilde{d}(u)\big)\tau - 2\log\bigg(\frac{\hat{c}(u) - e^{\tilde{d}(u)\tau}}{\hat{c}(u) - 1}\bigg)\bigg].
\end{aligned}$$

In summary, $\tilde{C}^j(u,t,T)$ and $\tilde{D}(u,t,T)$ have been represented as the second formulation in Lord and Kahl (2010).

Therefore, the characteristic function of x_m^j is given by

$$\begin{aligned}
\Phi^{\tilde{Q}}_{x_m^j}(u;t) &= \mathbb{E}^{\tilde{Q}}\left[e^{iux_m^j}|\mathcal{G}_t\right] = \Phi^j(u;t,m,x_m^j(t),V_t^j) \\
&= \exp\left\{iux_m^j(t) + \tilde{g}^j(u;t,m) + \tilde{D}(u;t,m)V_t^j\right\}, \quad t \in [m-1,m],
\end{aligned} \tag{B.44}$$

where

$$x_m^j(t) := \int_{m-1}^t \left(r_j + \frac{1}{2}V_s^j\right)ds + \int_{m-1}^t \sqrt{V_s^j}dW_s^{\tilde{Q}}, \tag{B.45}$$

and

$$\tilde{g}^j(u;t,m) := iur_j(m-t) + \tilde{C}^j(u;t,m). \tag{B.46}$$

Hence,

$$\begin{aligned}
\Phi^{\tilde{Q}}_{x_m}(u) &= \mathbb{E}^{\tilde{Q}}\left[e^{iux_m}\right] = \mathbb{E}^{\tilde{Q}}\left[\mathbb{E}^{\tilde{Q}}\left[e^{iux_m}|\mathcal{F}_{m-1}\right]\right] \\
&= \mathbb{E}^{\tilde{Q}}\left[e^{\tilde{D}(u;m-1,m)V_{m-1}}\left\langle\alpha_{m-1}, \tilde{\Psi}(u;m-1,m)1_n\right\rangle\right],
\end{aligned} \tag{B.47}$$

where $\tilde{\Psi}(u;t,m)$ is the fundamental solution of the following matrix-valued ODE:

$$\frac{d\tilde{\Psi}(u;t,m)}{dt} = \big[-\mathrm{Diag}(\tilde{G}(u;t,m)) + A\big]\tilde{\Psi}(u;t,m), \quad \tilde{\Psi}(u;m,m) = I_n \tag{B.48}$$

with

$$\tilde{G}(u;t,m) := \big(\tilde{g}_t^1(u;t,m), \tilde{g}_t^2(u;t,m), \ldots, \tilde{g}_t^n(u;t,m)\big)^\top$$

and

$$\begin{aligned}\tilde{g}_t^j(u;t,m) &= -iur_j - \frac{\kappa\theta_j}{\sigma_v^2}\left[(\kappa-(1+iu)\rho\sigma_v+\tilde{d}(u)) + \frac{2\tilde{c}(u)\tilde{d}(u)e^{\tilde{d}(u)(m-t)}}{1-\tilde{c}(u)e^{\tilde{d}(u)(m-t)}}\right] \\ &= -iur_j - \frac{\kappa\theta_j}{\sigma_v^2}\left[(\kappa-(1+iu)\rho\sigma_v+\tilde{d}(u)) + \frac{2\tilde{d}(u)e^{\tilde{d}(u)(m-t)}}{\hat{c}(u)-e^{\tilde{d}(u)(m-t)}}\right]. \end{aligned} \tag{B.49}$$

To further calculate (B.47), we next show

$$\mathbb{E}_t^{\tilde{Q}}\left[\alpha_T e^{uV_T}\right] = \tilde{\Pi}[u;t,T,\alpha_t]e^{\tilde{\Xi}(u;t,T)V_t}, \tag{B.50}$$

where $\tilde{\Pi}$ and $\tilde{\Xi}$ are two functions to be determined below.

In the same vein, we derive

$$\begin{aligned}
&d\big\{\tilde{\Pi}[u;t,T,\alpha_t]e^{\tilde{\Xi}(u;t,T)V_t}\big\} \\
&= e^{\tilde{\Xi}(u;t,T)V_t}\Big\{\tilde{\Pi}_t[u;t,T,\alpha_t]dt + \tilde{\Pi}[u;t,T]d\alpha_t \\
&\quad + \tilde{\Pi}[u;t,T,\alpha_t]\Big[\tilde{\Xi}_t(u;t,T)V_t dt + \tilde{\Xi}(u;t,T)dV_t + \frac{1}{2}\tilde{\Xi}^2(u;t,T)d\langle V_t,V_t\rangle\Big]\Big\} \\
&= e^{\tilde{\Xi}(u;t,T)V_t}\Big\{\Big[\tilde{\Pi}_t[u;t,T,\alpha_t] + \kappa\theta_{\alpha_t}\tilde{\Xi}(u;t,T)\tilde{\Pi}[u;t,T,\alpha_t] + \Big\langle\tilde{\Pi}[u;t,T],A\alpha_t\Big\rangle\Big]dt \\
&\quad + \tilde{\Pi}[u;t,T,\alpha_t]\Big[\tilde{\Xi}_t(u;t,T) + (\rho\sigma_v-\kappa)\tilde{\Xi}(u;t,T) + \frac{1}{2}\sigma_v^2\tilde{\Xi}^2(u;t,T)\Big]V_t dt \\
&\quad + \tilde{\Pi}[u;t,T,\alpha_t]\tilde{\Xi}(u;t,T)\sqrt{V_t}\sigma_v\big[\rho dW_t^{\tilde{Q}} + \sqrt{1-\rho^2}d\bar{W}_t^{\tilde{Q}}\big] + \Big\langle\tilde{\Pi}[u;t,T],dm_t\Big\rangle\Big\},
\end{aligned}$$

where

$$\tilde{\Pi}[u;t,T] := \big(\tilde{\Pi}[u;t,T,e_1],\tilde{\Pi}[u;t,T,e_2],\ldots,\tilde{\Pi}[u;t,T,e_n]\big)^\top \in \mathbb{R}^n. \tag{B.51}$$

Since $\tilde{\Pi}(u;t,T,\alpha_t)e^{\tilde{\Xi}(u;t,T)V_t}$ is a $\tilde{Q}$-martingale, setting the drift to be zero gives that $\tilde{\Pi}(u;t,T,e_j)$ and $\tilde{\Xi}(u;t,T)$ satisfy the following ODEs:

$$\tilde{\Pi}_t[u;t,T,e_j] + \kappa\theta_j\tilde{\Xi}(u;t,T)\tilde{\Pi}[u;t,T,e_j] + \Big\langle\tilde{\Pi}[u;t,T],Ae_j\Big\rangle = 0, \quad \tilde{\Pi}[u,T,T,e_j] = e_j, \tag{B.52}$$

and

$$\tilde{\Xi}_t(u;t,T) - \big(\kappa-\rho\sigma_v\big)\tilde{\Xi}(u;t,T) + \frac{1}{2}\sigma_v^2\tilde{\Xi}^2(u;t,T) = 0, \quad \tilde{\Xi}(u;T,T) = u. \tag{B.53}$$

Equation (B.53) is a Bernoulli equation with a complex terminal value, whose solution is given by

$$\tilde{\Xi}(u;t,T) = \begin{cases} \dfrac{2u}{-u\sigma_v^2\tau+2}, & \text{if } \kappa-\rho\sigma_v = 0, \\ \dfrac{2u(\kappa-\rho\sigma_v)}{-u\sigma_v^2(e^{(\kappa-\rho\sigma_v)\tau}-1)+2(\kappa-\rho\sigma_v)e^{(\kappa-\rho\sigma_v)\tau}}, & \text{if } \kappa-\rho\sigma_v \neq 0. \end{cases} \tag{B.54}$$

On the other hand, $\tilde{\Pi}[u;t,T]$ is the fundamental solution of the following matrix-valued ODE:

$$\frac{d\tilde{\Pi}[u;t,T]}{dt} = -\big\{\kappa\mathrm{Diag}[(\theta_1,\theta_2,\ldots,\theta_n)^\top]\tilde{\Xi}(u;t,T) + A\big\}\tilde{\Pi}[u;t,T], \quad \tilde{\Pi}[u;T,T] = I_n. \tag{B.55}$$

Hence, the solution of the first equation (B.52) is given by

$$\tilde{\Pi}[u;t,T,\alpha_t] = \Big\langle\alpha_t,\tilde{\Pi}[u;t,T]\Big\rangle. \tag{B.56}$$

Combining the above derivations gives

$$\begin{aligned}\Phi^{\tilde{Q}}_{x_m}(u) &= \mathbb{E}^{\tilde{Q}}\left[e^{\tilde{D}(u;m-1,m)V_{m-1}}\left\langle \alpha_{m-1}, \tilde{\Psi}(u,m-1)1_n\right\rangle\right] \\ &= e^{\tilde{\Xi}(\tilde{D}(u;m-1,m);0,m-1)V_0}\left\langle \alpha_0, \tilde{\Pi}[\tilde{D}(u;m-1,m);0,m-1]\tilde{\Psi}(u;m-1,m)1_n\right\rangle.\end{aligned}$$

Therefore,

$$\begin{aligned}\Phi_{Z_T}(u) &= \prod_{m=1}^{T}\Phi^{\tilde{Q}}_{x_m}\left(-u\frac{m}{T+1}\right) \\ &= \prod_{m=1}^{T} e^{\tilde{\Xi}\left(\tilde{D}\left(-u\frac{m}{T+1};m-1,m\right);0,m-1\right)V_0} \\ &\quad\times\left\langle \alpha_0, \tilde{\Pi}\left[\tilde{D}\left(-u\frac{m}{T+1};m-1,m\right);0,m-1\right]\tilde{\Psi}\left(-u\frac{m}{T+1};m-1,m\right)1_n\right\rangle \qquad \text{(B.57)}\end{aligned}$$

and the generalised characteristic function of Z_T is given by

$$\begin{aligned}\widehat{\Phi}_{Z_T}(\mathbf{c}(k),\mathbf{H}(k)) &:= \mathbb{E}^{\tilde{Q}}[e^{ic_T(k)Z_T}H_T(k)] \\ &= \mathbb{E}^{\tilde{Q}}\left[\mathbb{E}^{\tilde{Q}}\left[e^{ic_T(k)Z_T}H_T(k)|\alpha_T\right]\right] \\ &= \mathbb{E}^{\tilde{Q}}\left[\Phi_{Z_T}(c_T(k))H_T(k)\right] \\ &= \left\langle \exp\{\mathbf{A}\cdot T\}\alpha_0, \widehat{\mathbf{\Psi}}\right\rangle, \qquad \text{(B.58)}\end{aligned}$$

where $\widehat{\mathbf{\Psi}} = (\widehat{\Psi}_1, \widehat{\Psi}_2, \cdots, \widehat{\Psi}_n)^\top$ with

$$\begin{aligned}\widehat{\Psi}_j &= \prod_{m=1}^{T} e^{\tilde{\Xi}\left(\tilde{D}\left(-c_j(k)\frac{m}{T+1};m-1,m\right);0,m-1\right)V_0} \\ &\quad\times\left\langle \alpha_0, \tilde{\Pi}\left[\tilde{D}\left(-c_j(k)\frac{m}{T+1};m-1,m\right);0,m-1\right]\tilde{\Psi}\left(-c_j(k)\frac{m}{T+1};m-1,m\right)1_n\right\rangle H_j(k). \qquad \text{(B.59)}\end{aligned}$$